General Disclaimer

One or more of the Following Statements may affect this Document

- This document has been reproduced from the best copy furnished by the organizational source. It is being released in the interest of making available as much information as possible.

- This document may contain data, which exceeds the sheet parameters. It was furnished in this condition by the organizational source and is the best copy available.

- This document may contain tone-on-tone or color graphs, charts and/or pictures, which have been reproduced in black and white.

- This document is paginated as submitted by the original source.

- Portions of this document are not fully legible due to the historical nature of some of the material. However, it is the best reproduction available from the original submission.

RELEASED FOR ANNOUNCEMENT

IN NUCLEAR SCIENCE ABSTRACTS

WANL-TME-1384
FEBRUARY 28, 1966

CFSTI PRICES

H.C. $2.00; MN .50

SUBMITTED BY:

Westinghouse Electric Corporation
Astronuclear Laboratory
Pittsburgh, Pennsylvania 15236

PREPARATION OF MICROSCOPIC CROSS SECTIONS OF U^{235} FOR REACTOR CALCULATIONS

INFORMATION CATEGORY

UNCLASSIFIED

D. W. Drawbaugh 2/28/66
Authorized Classifier - Date

UNCLASSIFIED NERVA RESEARCH AND DEVELOPMENT REPORT.

PREPARED BY:

D. W. Drawbaugh

G. Gibson

M. M. Melnick
Reactor Physics & Mathematics

PREPARATION OF MICROSCOPIC CROSS SECTIONS OF U^{235} FOR REACTOR CALCULATIONS*

Donald W. Drawbaugh and Gordon Gibson
Westinghouse Astronuclear Laboratory

A set of resonance parameters for the epithermal range is given. The origin of these parameters is described. Of importance for reactor calculations is a table which gives the smooth (temperature independent) background cross sections which must be added in order to bring the single-level theoretical cross sections into agreement with experiment. The Saclay experimental data has been used; the corresponding Doppler broadening and experimental resolution have been taken into account in the calculations. This representation for the cross sections is of value for calculations concerning nuclear rocket reactors (NERVA) which operate at high temperatures, and for which a large fraction of the fissions are induced by epithermal neutrons.

I. INTRODUCTION

If for every pair of resonances the energy interval between the resonances is large as compared to the resonance level widths, the single level Breit-Wigner theory should be a good approximation. In this theory the fission and capture cross sections are composed of a series of resonances. If the parameters (resonance energies, and partial level widths) are known, the cross section may be obtained from a sum of Breit-Wigner terms. It is this theory with which we will be concerned.

Slowing-down programs which are used for obtaining flux averaged cross sections require the resonance parameters as input. It is important, of course, that the parameters which are used in these programs accurately represent the cross section. These programs take into account Doppler broadening of the resonances. Doppler broadening of the U^{235} resonances gives a significant contribution to the prompt temperature coefficient and the cold to hot reactivity change. To calculate such effects representation of the cross section through resonance parameters is important.

In general one cannot, from published experimental resonance parameters alone, obtain an adequate cross section representation. Further analysis is necessary, and it is this analysis which is described in this report. The published parameters are not a good representation for several reasons. In some instances resonances overlap, i.e. they cannot be resolved experimentally and no shape analysis has been carried out so the level widths are not available. Yet these resonances cannot be

*Work performed under the auspices of the Space Nuclear Propulsion Office. Prime Contractor Aerojet-General Corporation.

neglected. Some information is often available from an area analysis so that under various assumptions some estimate of a level width may be made. In other instances even this cannot be done. In either case it is necessary to compare the experimental cross section in this energy interval with the theoretical cross section calculated from the resonances in the cross section library. In this way some smooth background cross section (which is independent of the temperature) can be added so that all of the cross section is included in the library. In general this is an adequate representation since when resonances overlap the equivalent of a broad resonance is formed and the Doppler effects tend to be small. Of course multilevel theory is required for an accurate treatment in these cases. Even when the resonances are well separated, if one takes the published resonance parameters and folds in the Doppler broadening and counter resolution some smooth background cross section must be added to that calculated from the resonances before agreement with experimental data is obtained. Finally, the parameters determined by different experimentalists vary considerably and their measurements have been made over different energy ranges thus, only by a study of this kind can a consistent selection of parameters be made.

We have accepted the Saclay[1] experimental data over most of the energy range studied (1.86 eV to 37.3 eV). We also started with the resonance parameters given by Michaudon[1] supplemented by parameters given in the recent Brookhaven Sigma Center compilation[2]. In many cases a new determination of parameters was made where none were suggested, or when the suggested parameters gave a poor fit to the Saclay data. The parameters were varied, attempting to stay within the suggested ranges, to fit the Saclay data. Above 37.3 eV we have used a statistical model plus smooth (temperature independent) cross section to fit the experimental data. This "unresolved range" above 37.3 eV will not be discussed further in this report. Our primary concern is not a precise shape analysis but, rather, an adequate representation for all of the cross section.

Much of the analysis and computer code tools have been described in previous reports[3,4]. The analysis reported here contains several improvements. We have used the data compiled on magnetic tape by the Brookhaven National Laboratory Sigma Center[5] and have taken account of experimental resolution.

II. DISCUSSION OF DOPPLER BROADENING AND EXPERIMENTAL RESOLUTION

Consider a beam of neutrons incident on a U^{235} target. The target nucleii are in thermal motion characterized by the temperature of the solid. If the resultant particles from a particular reaction are observed directly, e.g. as when the fission process occurs, the effective cross section σ^e may be determined from

$$\frac{dn}{dt} = n\rho\sigma^e v = J\rho\sigma^e ,$$

or

$$R = \frac{dn}{dt} AL = (JA)(\rho L)\sigma^e = ID\sigma^e$$

Therefore, $\sigma^e = \frac{R}{ID}$, where (1)

$R = AL \frac{dn}{dt}$ (sec^{-1}) is the rate at which events occur,

$D = \rho L$ (cm^{-2}) is the area density of target nucleii.

$I = JA$ (sec^{-1}) is the current of neutrons in the beam,

$\vec{v}$ ($cm\ sec^{-1}$) is the velocity of neutrons in the beam,

n (cm^{-3}) is the density of neutrons in the beam,

A is the area of the beam,

and L is the target thickness.

Theoretically the effective cross section can be expressed as

$$\sigma^{e}_{D.B.} = \frac{1}{v}\int \left|\vec{v} - \vec{V}\right| \sigma\left(\left|\vec{v} - \vec{V}\right|\right) f(\vec{V})\, d\vec{V}\ , \qquad (2)$$

where $\vec{V}$ is the velocity of a target nucleus,

$f(\vec{V})$ is the distribution of the velocities $\vec{V}$,

and σ is the nuclear cross section for the reaction.

The EXT program[6] has been developed at the Westinghouse Astronuclear Laboratory for determining the effective cross section for a target at temperature T when given the resonance parameters (which pertain to a zero temperature target). EXT treats s wave neutrons only; it includes interference between potential and resonance scattering, but not interference between levels. A Maxwellian velocity distribution is assumed for the target nucleii. If the nucleii are in thermal motion in solid U^{235} at ambient temperature (Debye temperature for Uranium is $\approx 200°K$), an effective temperature[7] T^e which is ~ 2 percent greater[1] than the target temperature should be used in the Maxwell distribution. This compensates for the crystalline binding effects. For Uranium at 77°K (Debye temperature[1] $\approx 160°K$) an effective temperature of $\approx 87°K$ should be used in the Maxwellian distribution.

If $V \ll v$ so that $\left|\vec{v} - \vec{V}\right| \cong v$ (this approximation[8] has not been made in the EXT program), the energy E' associated with the relative velocity $\vec{v} - \vec{V}$ in the C.M. coordinate system can be expanded in powers of V/v, i.e. if $E' = \frac{1}{2}\mu\left|\vec{v} - \vec{V}\right|^2$ where $\mu = \frac{A}{A+1}\, m$, m is the mass of the neutron, A is the mass number of the target nucleus, and if $\vec{v}$ is in the z direction then

$$E' \cong \tfrac{1}{2}\mu v^2 - \mu v\, V_z\ ,$$

or

$$E' = E - (2\mu E)^{\frac{1}{2}} V_z \quad \text{and} \quad V_z = \frac{E - E'}{(2\mu E)^{\frac{1}{2}}}\ .$$

Since $\left|\vec{v} - \vec{V}\right|$ is a function only of V_z in this approximation, the three-dimensional distribution function in Equation 2 may be replaced by a one-dimensional distribution. Hence Equation 2 becomes:

$$\sigma^{e}_{D.B.} \cong \int \sigma\left(\left|\vec{v} - \vec{V}\right|\right) f(V_z)\, d V_z\ ,$$

where

$$f(V_z)dV_z = \sqrt{\frac{M}{2\pi kT^e}}\ e^{-\frac{M V_z^2}{2kT^e}}\, d V_z\ ,$$

M is the absorber mass, and kT^e is the effective kinetic temperature of the target nucleii.

Therefore

$$\sigma^{e}_{D.B.}(E) = \sqrt{\frac{M}{2\pi kT^e}} \int \sigma(E')\, e^{-\frac{M(E-E')^2}{2\mu E 2kT^e}} \left(\frac{dE'}{\sqrt{2\mu E'}}\right)$$

and if $\Delta = \sqrt{\frac{4\mu kT^e E}{M}}$,

$$\sigma^e_{D.B.}(E) = \frac{1}{\sqrt{\pi}\Delta} \int \sigma(E')\, e^{-\left(\frac{E'-E}{\Delta}\right)^2} dE' \,. \qquad (3)$$

Hence as is well known the Doppler broadened cross section, $\sigma^e_{D.B.}$, can be computed by convoluting the nuclear cross section, σ, and a Gaussian function. In the lab coordinate system Equation 3 holds if

$\Delta = \sqrt{\frac{4kT^e E}{A}}$ and E is the energy in the lab frame.

In obtaining the experimental data resonances are further broadened by the finite resolution of the detection system. The resolution function is discussed in Appendix 1. To take this into account, the Doppler broadened cross section given by Equation 3 must be further convoluted with the experimental response function R(E"-E), i.e.

$$\sigma^e(E) = \int \sigma^e_{D.B.}(E'')\, R(E''-E)\, dE''.$$

If the resolution function is Gaussian

$$R(E''-E) = \frac{1}{\sqrt{\pi}\delta}\, e^{-\left(\frac{E''-E}{\delta}\right)^2} ,$$

$$\text{then} \quad \sigma^e(E) = \frac{1}{\pi\delta\Delta} \int \left[\int \sigma(E')\, e^{-\left(\frac{E'-E''}{\Delta}\right)^2} dE' \right] e^{-\left(\frac{E''-E}{\delta}\right)^2} dE'',$$

$$\text{or} \quad \sigma^e(E) = \frac{1}{\sqrt{\pi}\sqrt{\delta^2+\Delta^2}} \int \sigma(\xi)\, e^{-\frac{(\xi-E)^2}{\Delta^2+\delta^2}} d\xi \qquad (4)$$

since successive convolutions with two Gaussians is equivalent to convoluting with a single Gaussian having a width given by the square root of the sum of the squares of the widths of the two original Gaussians.

Summarizing, the effects of both Doppler broadening and counter resolution are equivalent to just Doppler broadening where the temperature to be used in determining the velocity distribution function of the target nucleii is

$$T = \frac{A}{4kE}(\Delta^2 + \delta^2) = T^e + T^R \qquad (5)$$

where $T^R = \frac{A\delta^2}{4kE}$, and T^e is the effective temperature defined previously.

The effective total cross section, σ^e_t, as a function of neutron energy, E, is determined from transmission measurements. In transmission experiments a beam of neutrons passes through a target and the counting rate, I, of the neutrons remaining in the beam after transmission are detected as a function of neutron energy. If the counting rate with no target is I_o then

$$t(E) = \frac{I(E)}{I_o(E)} = e^{-D\sigma^e_t(E)} \,. \qquad (6)$$

It has been shown that Doppler broadening follows a Gaussian function so the theoretical Doppler broadened total cross section is given by

$$\sigma_{t_{D.B.}}(E') = \frac{1}{\Delta\sqrt{\pi}} \int_0^\infty \sigma_t(E'')\, e^{-\left(\frac{E''-E'}{\Delta}\right)^2} dE''$$

hence

$$t_{D.B.}(E') = e^{-D\sigma_{t_{D.B.}}(E')} \qquad (7)$$

If the detection response function is Gaussian, then the theoretical

transmission which is to be compared with the experimental transmission is

$$t(E) = \frac{1}{\delta(E)\sqrt{\pi}} \int_0^\infty t_{D.B.}(E')\, e^{-(\frac{E-E'}{\delta})^2}\, dE'$$

or

$$t(E) = \frac{1}{\delta(E)\,\pi} \int_0^\infty e^{-D\sigma_{t_{D.B.}}(E')} e^{-(\frac{E-E'}{\delta})^2}\, dE' \quad . \tag{8}$$

From ó and 8 we may write

$$e^{-D\,\sigma_t^e(E)} = \frac{1}{\delta\sqrt{\pi}} \int_0^\infty e^{-D\sigma_{t_{D.B.}}(E')}\, e^{-(\frac{E-E'}{\delta})^2}\, dE'$$

for thin targets $D \to 0$ ("thin" means the target thickness << mean free path) and

$$1-D\,\sigma_t^e(E) = \frac{1}{\delta\sqrt{\pi}} \int_0^\infty \left[1-D\sigma_{t_{D.B.}}(E')\right] e^{-(\frac{E-E'}{\delta})^2}\, dE'$$

or

$$1-D\,\sigma_t^e(E) = 1 - \frac{D}{\delta\Delta\pi} \int_0^\infty \left[\int_0^\infty \sigma_t(E'')\, e^{-(\frac{E''-E'}{\Delta})^2}\, dE''\right] e^{-(\frac{E-E'}{\delta})^2} dE'$$

or

$$\sigma_t^e(E) = \frac{1}{\sqrt{\pi}\,\sqrt{\delta^2+\Delta^2}} \int_0^\infty \sigma_t(\xi')\, e^{-\frac{(E-\xi')^2}{\Delta^2+\delta^2}}\, d\xi' \tag{9}$$

similar to the expression for the effective fission cross section.

As before, under the assumption of a thin target, the experimental resolution has the effect of enhancing[9] the Doppler broadening and can be taken into account by using the "target temperature" T given by Equation 5.

III. CALCULATIONS AND RESULTS

Given a set of experimental (effective cross section) data one must in effect unfold the Doppler broadening and counter resolution from Equations 4 and 9 to obtain the nuclear cross sections. We have chosen Michaudon's[1] fission and total cross section measurements for the analysis. These are available in the SCISRS library[5].

The fission data was obtained with the Uranium at ambient temperature, and the total cross section with the Uranium at the temperature of liquid nitrogen. The temperatures to be used as input to EXT were obtained from Equation 5. For the fission data $kT^e = .02637$ ev, for the total cross section data $kT^e = .00758$. In Appendix I the method of determining the resolution, δ, for the Saclay linear accelerator time-of-flight facility is described. Figure 1 is a plot of kT^R as a function of neutron energy under the experimental conditions existing when the fission cross section data was obtained. Figure 2 is a plot of kT^R for the total cross section data as a function of neutron energy. Table I gives the kinetic temperatures that were used in the calculation as a function of neutron energy for the fission and total cross section calculations.

By trial-and-error (the method for selecting the resonance parameters to input into EXT is described in the introduction) a set of parameters has been obtained that yields cross sections which agree in general quite well with the experimental data when in addition to the resonances smooth background fission cross section of the form

$$\sigma_f^{sm}(bg) = \sigma_f^o \sqrt{\frac{.0253\ ev}{E}} \tag{10}$$

is added in various energy intervals. Values of σ_f^o are given in Table I. Also, a background contribution from a negative energy resonance of the form

$$\sigma^{sm}(N.R.) = \frac{K}{\sqrt{E}\,(E-E_o)^2} \qquad (11)$$

has been added. The parameters for the negative energy resonance are $E_o = -1.45$ eV, $K_{fission} = 176.79$, and $K_{capture} = 31.71$ corresponding to $\Gamma_\gamma = 40 \times 10^{-3}$ eV and $\Gamma_f = 223 \times 10^{-3}$ eV. Values for this contribution to the cross sections is given in Table III. It is worth noting that no background capture cross section (other than the negative energy resonance contribution) has been added. One would expect that the fission cross sections would need adjustment since statistical analyses[10] of the fission widths indicate only a couple of exit channels for the reaction, hence interference does occur. There are many exit channels for the capture process however, and interference effects should not be present. Since there are many exit channels the partial level widths for capture should not vary greatly from resonance to resonance. When this partial width has not been determined experimentally for a level we have chosen $\Gamma_\gamma = 40 \times 10^{-3}$ eV unless our shape analysis has forced a change in this value. The set of resonance parameters we have obtained to represent the cross section are given in Table II.

For each temperature, 10 minutes of computer (IBM-7094) time is required to calculate the cross sections from 1.86 - 37.3 eV. For a given energy, E, all the resonances included in the energy interval E $\pm$ 10 eV are assumed to contribute to the cross section. In the trial-and-error portion of the calculation for initially determining the resonance parameters only the contribution from a few of the neighboring resonances was considered.

The smooth curves in Figures 5 through 13 are the theoretical fission cross sections which have been calculated for our set of resonances and they include the background (Equations 10 and 11) cross sections. The experimental cross section values of Saclay denoted by the symbol, x, on the plots were obtained from the SCISRS[5] library. Through the RETREV[5] program which secures these particular cross sections from the library, the Curve Plot for SCISRS[11] program stored the energy and cross section values on sublibrary tapes. These tapes are then compatable for use with a program, CalComp for SCISRS (CCS), written especially to produce plots by means of the CalComp model 556 digital incremental plotter.

The circled experimental points have been multiplied by 1/10. The theoretical values for the cross section at some of the resonance peaks have also been multiplied by 1/10. The Saclay experimental fission cross section was not available for energies below ~7 eV. Figures 3 and 4 compare the theoretical fission cross section with the experimental data given in BNL-325 supplement 2. As can be seen in Figure 1 the experimental resolution has a negligible effect on the data over this energy range.

Figures 14 through 24 are the total cross sections as a function of energy. The theoretical curves include the fission and capture resonance cross sections, the resonance, potential, and interference term for the scattering cross section, as well as the background fission cross section (Equation 10) and the contribution to the fission and capture cross sections due to the negative energy resonance (Equation 11).

In the energy interval of ~ 24.3 eV - 25.6 eV there are ~ three unresolved resonances. We have not chosen to select parameters for these resonances, but have added this cross section as a smooth background cross section.

No resonances have been considered for energies > 37.3 eV, which is the upper limit of the energy interval analyzed. Above this energy it is difficult in general to resolve the resonances. In the interval ~35.5 eV to 37.3 eV some smooth fission cross section has been added to the calculated cross section in order to bring the theoretical and experimental cross sections into agreement.

The resonance parameters are put into the cross section library; in addition, the smooth background cross section must be added. To find the average smooth background cross section $\langle\sigma^{sm}\rangle$ to be added in an energy range E_L to E_u corresponding to a lethargy interval of $\frac{1}{4}$, we have used:

$$\langle\sigma_f^{sm}\rangle = 4\int_{E_L}^{E_u} \sigma_f^{sm} \frac{dE}{E} . \qquad (12)$$

For the background terms of the form given by Equation 10

$$\langle\sigma_f^{sm}(bg)\rangle = 8\ \sigma_f^{\circ}\ \sqrt{.0253\ eV}\ \left[\frac{1}{\sqrt{E_L}} - \frac{1}{\sqrt{E_u}}\right] , \qquad (13)$$

and the calculated values are given in Table III.

For the background due to the negative resonance given by Equation 11, i.e.

$$\sigma^{sm}(N.R.) = \frac{K}{\sqrt{E}\ (E-E_o)^2} = \frac{K}{\sqrt{E}\ (E+|E_o|)^2} ,$$

$$\langle\sigma^{sm}(N.R.)\rangle = \frac{-8K}{(|E_o|)^{5/2}} \left\{\frac{1}{\chi} + \frac{1}{2}\frac{\chi}{\chi^2+1} + \frac{3}{2}\tan^{-1}\chi\right\}_{\sqrt{\frac{E_L}{|E_o|}}}^{\sqrt{\frac{E_u}{|E_o|}}} \qquad (14)$$

and the calculated values are given in Table III for both the fission and capture cross sections.

For the background that must still be added to account for "missing fission cross section", i.e. due to the omission of resonances (e.g. see Figure 10):

$$\sigma_f^{sm}(m) = \sigma_f^{exp} - \sigma_f^{theo}, \text{ where } \sigma_f^{theo} \text{ includes} \qquad (15)$$

the contributions from terms given by Equation 10 and 11. Equation 15 is substituted into Equation 12 which is then solved numerically. The results are also given in Table III. Similarly for the capture cross section,

$$\sigma_c^{sm}(m) = \sigma_{total}^{exp} - (\sigma_{total}^{theo} + \sigma_f^{sm}(m)) \quad (\text{where } \sigma_{total}^{theo} \qquad (16)$$

is the theoretical cross section shown in Figures 14 through 24) is substituted into Equation 12 which is solved numerically. In addition to accounting for the omission of resonances some missing capture cross section (of small magnitude) must be added over a few energy intervals where the experimental and theoretical total cross sections do not agree. For energy group 53 (see Table III) where the theoretical cross section is higher than the experimental, some smooth capture cross section must be subtracted.

In this portion of the calculation it has been assumed that except at the resonances the scattering cross section is essentially due to potential scattering (~12 barns) and is properly accounted for. At resonances it

is assumed that the resonance scattering cross section is small relative to the fission and capture cross sections. Hence having matched the theoretical and experimental fission cross sections, it has been assumed that deviations between the theoretical and experimental total cross section are due to the theoretical capture cross section.

IV. CONCLUSIONS

An analysis of the type presented in this paper is necessary to obtain a cross section library for reactor calculations that is a good representation of the actual cross section. Without the analysis there is no good method for selecting a consistent set of parameters, for accounting for missing resonances, for treating the background cross section, or for accounting for deviations from single level theory. Part of the analysis necessitates repetition of calculations which must already have been done to obtain the resonance parameters from the experimental data. It would be of considerable help to the "user" of cross sections if when a set of resonance parameters are given the analyst would show the cross section (Figures 3-24) which these resonance parameters would produce under the experimental conditions and compare this information with the experimental cross section.

V. ACKNOWLEDGMENTS

The computer code XO and EXT and the plotting codes were ably programmed by Marian Melnick. Dr. John Stehn and Mr. J. Friedman of the Brookhaven National Laboratory have been most helpful in supplying updated versions of the SCISRS data file.

Table I Parameter For Obtaining Background Fission Cross Section, and Temperatures ($T^e + T^R$) That Are Used For the "Doppler Broadening" Calculation.

Energy Interval ΔE(ev)	Background Fission Cross Section Parameter σ_f^o(barns)	Kinetic Temperature For Obtaining Total Cross Section kT(ev)	Kinetic Temperature For Obtaining Fission Cross Section kT(ev)
1.85- 8.95	-	.0079	.0265
9.00-10.95	234	.0077	.0266
11.00-14.30	222	.0078	.0267
14.35-18.95	87.5	.0079	.0268
19.00-19.95	360	.0080	.0268
20.00-24.95	270	.0081	.0270
25.00-28.95	270	.0082	.0272
29.00-33.95	172	.0084	.0273
34.00-37.3	172	.0087	.0276

Table II U^{235} Resonance Parameters

No.	E(ev)	$\Gamma_n(10^{-3}ev)$	$\Gamma_f(10^{-3}ev)$	$\Gamma_a(10^{-3}ev)$	NR=2 NRIA=1
1	0.273	.0032	100	135	1
2	1.135	.0154	115	157	1
3	2.04	.0077	10	47	1
4	2.89	.005	100	140	1
5	3.15	.023	100	137	1
6	3.61	.047	45	87	1
7	4.85	.056	3.8	40.8	2
8	5.48	.022	330	370	1
9	5.84	.012	150	195	1
10	6.20	.042	130	170	1
11	6.40	.260	10	45	2
12	7.095	.120	28	64	2
13	8.795	1.18	82	132	1
14	9.28	.20	95	160	1
15	9.74	.04	140	180	1
16	10.18	.06	58	95	2
17	11.65	.63	4	40	2
18	12.39	1.29	24	68	2
19	12.86	.04	60	83	2
20	13.28	.04	51	91	2
21	13.71	.044	70	110	2
22	14.00	.42	400	440	1
23	14.53	.115	23	61	2
24	15.415	.250	49	98	2
25	16.095	.350	17	52	2
26	16.68	.265	86	132	2
27	18.05	.39	90	160	2
28	18.97	.10	25	65	2
29	19.29	3.1	52	102	2
30	20.13	.13	65	120	2
31	20.60	.23	33	92	2
32	21.06	1.58	21	68	2
33	22.93	.45	42	92	2
34	23.41	.69	8	40	2
35	23.61	.80	85	165	2
36	24.27	.33	52	92	2
37	25.62	.44	150	190	2
38	26.49	.43	150	190	2
39	27.05	.10	200	240	2
40	27.79	.76	60	123	2
41	28.34	.16	96	140	2
42	29.63	.18	22	67	2
43	30.59	.21	77	150	2
44	30.85	.49	17	59	2
45	32.06	1.95	38	90	2
46	33.51	1.80	20	60	2
47	34.38	1.80	40	90	2
48	34.81	1.05	49	109	2
49	35.19	4.30	120	183	2

Table III Smooth Cross Sections Which Must Be Added To Each GAM Group In Addition To The Resonance Cross Sections

Energy Group	Energy Interval ev	Fission Background Cross Section $\langle\sigma_f^{sm}(bg)\rangle$(barns)	Negative Energy Resonance $\langle\sigma^{sm}(N.R.)\rangle$(barns)	Missing Cross Section $\langle\sigma^{sm}(m)\rangle$(barns)	Total Smooth Fission Cross Section Added $\langle\sigma_f^{sm}\rangle$(barns)	Total Smooth Absorption Cross Section Added $\langle\sigma_a^{sm}\rangle$(barns)
62	1.86- 2.38	0	$\sigma_f = 9.57$ $\sigma_\gamma = 1.72$		9.57	11.29
61	2.38- 3.06	0	$\sigma_f = 6.33$ $\sigma_\gamma = 1.13$		6.33	7.46
60	3.06- 3.93	0	$\sigma_f = 3.96$ $\sigma_\gamma = 0.71$	$\sigma_\gamma = 1.1$	3.96	5.77
59	3.93- 5.04	0	$\sigma_f = 2.42$ $\sigma_\gamma = 0.43$		2.42	2.85
58	5.04- 6.48	0	$\sigma_f = 1.46$ $\sigma_\gamma = 0.26$		1.46	1.72
57	6.48- 8.32	0	$\sigma_f = 0.85$ $\sigma_\gamma = 0.15$		0.85	1.00
56	8.32-10.68	8.12	$\sigma_f = 0.17$ $\sigma_\gamma = 0.03$		8.29	8.32
55	10.68-13.7	10.2			10.2	10.2
54	13.7 -17.6	4.57		$\sigma_f = 0.4$ $\sigma_\gamma = 0.9$	4.97	5.87
53	17.6 -22.6	8.21		$\sigma_\gamma = -2.8$	8.21	5.41
52	22.6 -29.0	8.49		$\sigma_f = 4.50$ $\sigma_\gamma = .68$	12.99	13.67
51	29.0 - 37.3	4.77		$\sigma_f = 2.94$ $\sigma_\gamma = 1.44$	7.71	9.15

APPENDIX I - THE EXPERIMENTAL RESOLUTION

The three principal causes of the experimental resolution broadening are:

1) the duration of the fast neutron burst τ_1
2) the detector gate time τ_2
3) the moderation time; that is, the time required for the fast neutrons to slow down in the target to the energy E.

Each of the contributions has a certain distribution in time (or in energy), and the resolution function is the triple convolution of the three distributions. It is usual to consider each of the first two contributions to be rectangular.

The convolution of two rectangular distributions is a trapezoidal distribution (or triangular when $\tau_1 = \tau_2$).

The moderation time in an infinite medium is derived in reference 1, p. 25. The same formula has been derived in a different manner by Groenewold and Geoendyk[12]. The distribution function in time of neutrons whose energies have been moderated to energy E is

$$\psi(t) = \tfrac{1}{2} k^3 t^2 e^{-kt}.$$

Then

$$\int_0^\infty \psi(t)\, dt = 1 ,$$

$$\int_0^\infty t\psi(t)\, dt = \frac{3}{k} ,$$

$$\int_0^\infty t^2\psi(t)\, dt = \frac{12}{k^2} ,$$

where $k = \frac{1}{\tau_m}$ and τ_m is the mean collision time of a neutron of energy E with a proton in the moderator. The variance σ^2 of the distribution is

$$\sigma^2 = \frac{12}{k^2} - \frac{9}{k^2} = \frac{3}{k^2} .$$

The convolution of two normalized rectangular distributions of base τ_1 and τ_2 gives a normalized trapezoidal distribution. The convolution, R(t), of this trapezoidal distribution with the distribution $\psi(t)$ can be integrated. The result is as follows. Putting

$$\tfrac{1}{2}(\tau_1 + \tau_2) = a$$

$$\tfrac{1}{2}(\tau_2 - \tau_1) = b$$

(always choosing τ_2 to be the larger of τ_2 and τ_1 if they are not equal). And

$$I_1(t) = \int \psi(t')dt' = -e^{-kt}\left[+1+kt+\frac{k^2t^2}{2}\right] ,$$

$$I_2(t) = \int t'\psi(t')dt' = -e^{-kt}\left[\frac{3}{k} + 3t + \frac{3}{2}kt^2 + \frac{k^2t^3}{2}\right]$$

The result is:

<u>for</u> $0 < t + a \leq \tau_1$

$$R = \frac{t + a}{\tau_2 \tau_1}\left[I_1(t+a) - I_1(0)\right]$$

$$- \frac{1}{\tau_2 \tau_1} \left[I_2(t+a) - I_2(0) \right]$$

For $\tau_1 - a < t \leq b$

$$R = \frac{t+a}{\tau_2 \tau_1} \left[I_1(t+a) - I_1(t+b) \right]$$

$$- \frac{1}{\tau_2 \tau_1} \left[I_2(t+a) - I_2(t+a) \right]$$

$$+ \frac{1}{\tau_2} \left[I_1(t+b) - I_1(0) \right]$$

For $b < t \leq a$

$$R = \frac{t+a}{\tau_2 \tau_1} \left[I_1(t+a) - I_1(t+b) \right]$$

$$- \frac{1}{\tau_2 \tau_1} \left[I_2(t+a) - I_2(t+b) \right]$$

$$+ \frac{1}{\tau_2} \left[I_1(t+b) - I_1(t-b) \right]$$

$$- \frac{t-a}{\tau_2 \tau_1} \left[I_1(t-b) - I_1(0) \right]$$

$$+ \frac{1}{\tau_2 \tau_1} \left[I_2(t-b) - I_2(0) \right]$$

For $a < t$

$$R = \frac{t+a}{\tau_2 \tau_1} \left[I_1(t+a) - I_1(t+b) \right]$$

$$- \frac{1}{\tau_2 \tau_1} \left[I_2(t+a) - I_2(t+b) \right]$$

$$+ \frac{1}{\tau_2} \left[I_1(t+b) - I_1(t-b) \right]$$

$$- \frac{t-a}{\tau_1 \tau_2} \left[I_1(t-b) - I_1(t-a) \right]$$

$$+ \frac{1}{\tau_1 \tau_2} \left[I_2(t-b) - I_2(t-a) \right]$$

Using this formula with $\tau_1 = \tau_2$ the resolution function R(t) has been computed and plotted for various values of k. The resulting family of curves was compared and showed agreement with the curves - Figure B.2.15 page 286 of Michaudon's thesis[1].

A computer program was written to compute numerical values of R(t). For each resolution function R(t) two Gaussian distributions $G_1(t)$ and $G_2(t)$ are computed. The distribution $G_1(t)$ has the same average and variance as R(t). The distribution $G_2(t)$ has the same width at half-maximum as

R(t) and is positioned at the center of the width at half maximum of R(t).

Some comparisons of plots of $G_1(t)$ and $G_2(t)$ with R(t) were made. From these comparisons it was concluded that use of a Gaussian distribution with the same variance $\frac{1}{2}\delta^2$ as R(t) gave an adequate representation of R(t). It should be pointed out that there are other contributions to the resolution function beside the three chief ones mentioned above. The convolution of these additional effects with the first three will tend to make the resolution function approach a Gaussian. This is discussed in Michaudon's thesis, page 55.

Parameters in the resolution function:

1) Fission Cross Section Measurements - From the table Figure C.2.6 page 306 of Michaudon's thesis the burst time $\tau_1 = .5\mu$ sec. and the detector time $\tau_2 = .5\mu$ sec. over the energy range from 7 to 96 eV. These numbers are in agreement with with τ_1 and τ_2 printed out from the SCISRS data tape for the Michaudon fission data. (Reference CEA-2552 in the SCISRS Printout.)

From page 54 of reference 1 we learn that the target for the fission data was nylon and that for nylon the mean collision time with hydrogen is

$$\tau_\infty(\mu\text{sec}) = \frac{0.55}{\sqrt{E(eV)}}$$

where τ_∞ is for an infinite medium. To account for the finite target size Michaudon found from Monte Carlo calculations that the infinite medium standard deviation should be multiplied by 2/3 to get the standard deviation for the finite target (reference 1, page 56). This means

$$\tau = (\tfrac{2}{3})\tau_\infty = \frac{2}{3} \times \frac{0.55}{\sqrt{E(eV)}}$$

or

$$k = \frac{1}{\tau} = \frac{3}{2} \frac{\sqrt{E(eV)}}{0.55}$$

For the fission measurements the flight path was 52.08 meters (reference 1, page 306).

The fission cross section data on the SCISRS data tape is for the sample at ambient temperature.

2) Total Cross Section Measurements - From the table Figure C.3.8 page 319 of reference 1 we find for the energy range 1.3 to 7.7 eV that the accelerator burst time was 2μsec., the detector time 2μ sec. However, the values for these parameters printed out from the SCISRS data tape were burst time 1μ sec. and detector time 2μ sec. We have used the latter values presuming that the SCISRS data is different from that presented in reference 1 for this range and that the parameters listed in the SCISRS library are correct for the corresponding data.

For the energy range 7.2 to 50 eV the parameters given in reference 1 are burst time 0.5μ sec. and detector time 0.5μ sec. These agree for this energy range with the values printed out from the SCISRS data tape. The flight path for both energy ranges is printed out from the SCISRS data tape to be 53.71 meters. The total cross section measurements analyzed were made at 77°K.

To convert the resolution in time to resolution in energy:

$$\delta(E) = 2.76 \times 10^{-2} \frac{\delta(t)}{L} E^{3/2}$$

where E is in eV, L is in meters, and t is in μ sec. (reference 1, page 26).

To obtain this result:

$$t = \frac{L}{v} = \frac{\ell}{\sqrt{\frac{2E}{m}}} \quad \text{or} \quad E = \frac{mL^2}{2}\,\frac{1}{t^2}$$

$$\delta(E) = -\frac{2^{3/2}}{\sqrt{m}}\,\frac{\delta(t)}{L}\,E^{3/2}$$

For the units given above:

$$\delta(E) = \frac{2^{3/2} \times 10^{-6} \times 10^{-2}\ \sqrt{1.602}\ \times 10^{-6}}{\sqrt{1.660}\ 10\text{-}12}\,\frac{\delta(t)}{L}\,E^{3/2}$$

or

$$\delta(E) = 2.76 \times 10^{-2}\,\frac{\delta(t)}{L}\,E^{3/2}$$

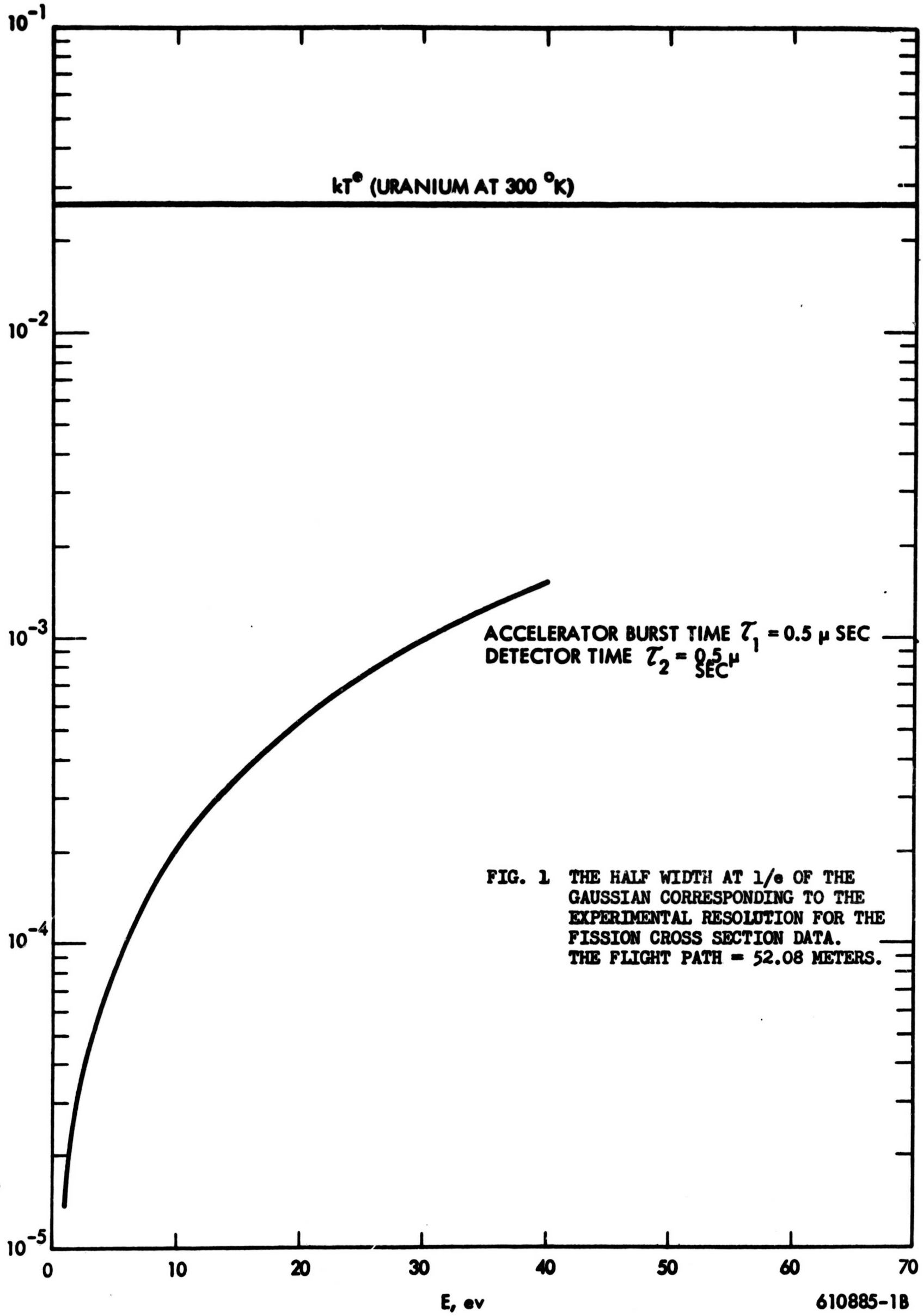

FIG. 1 THE HALF WIDTH AT 1/e OF THE GAUSSIAN CORRESPONDING TO THE EXPERIMENTAL RESOLUTION FOR THE FISSION CROSS SECTION DATA. THE FLIGHT PATH = 52.08 METERS.

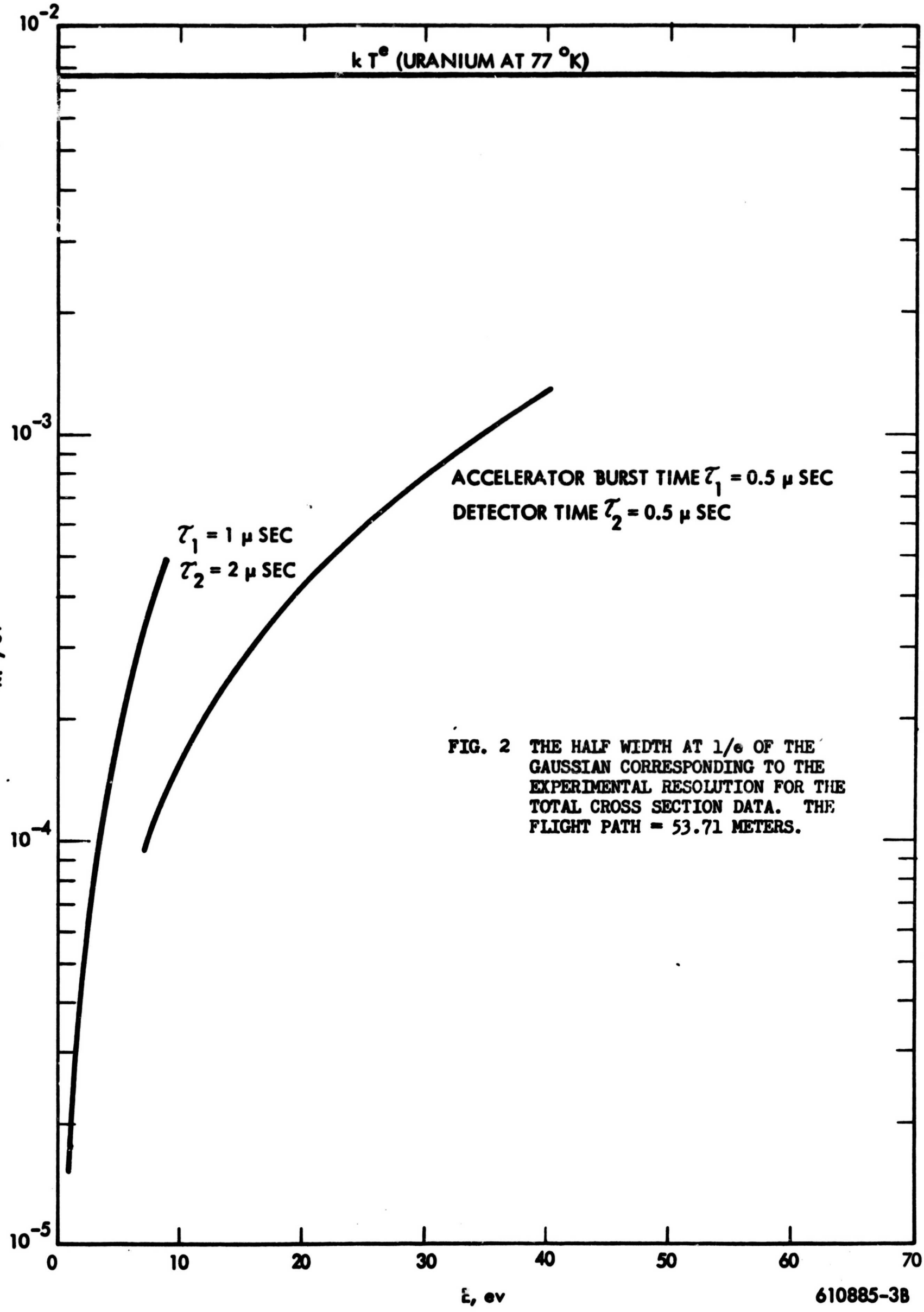

FIG. 2 THE HALF WIDTH AT 1/e OF THE GAUSSIAN CORRESPONDING TO THE EXPERIMENTAL RESOLUTION FOR THE TOTAL CROSS SECTION DATA. THE FLIGHT PATH = 53.71 METERS.

FIG. 3 FISSION CROSS SECTION FOR U-235

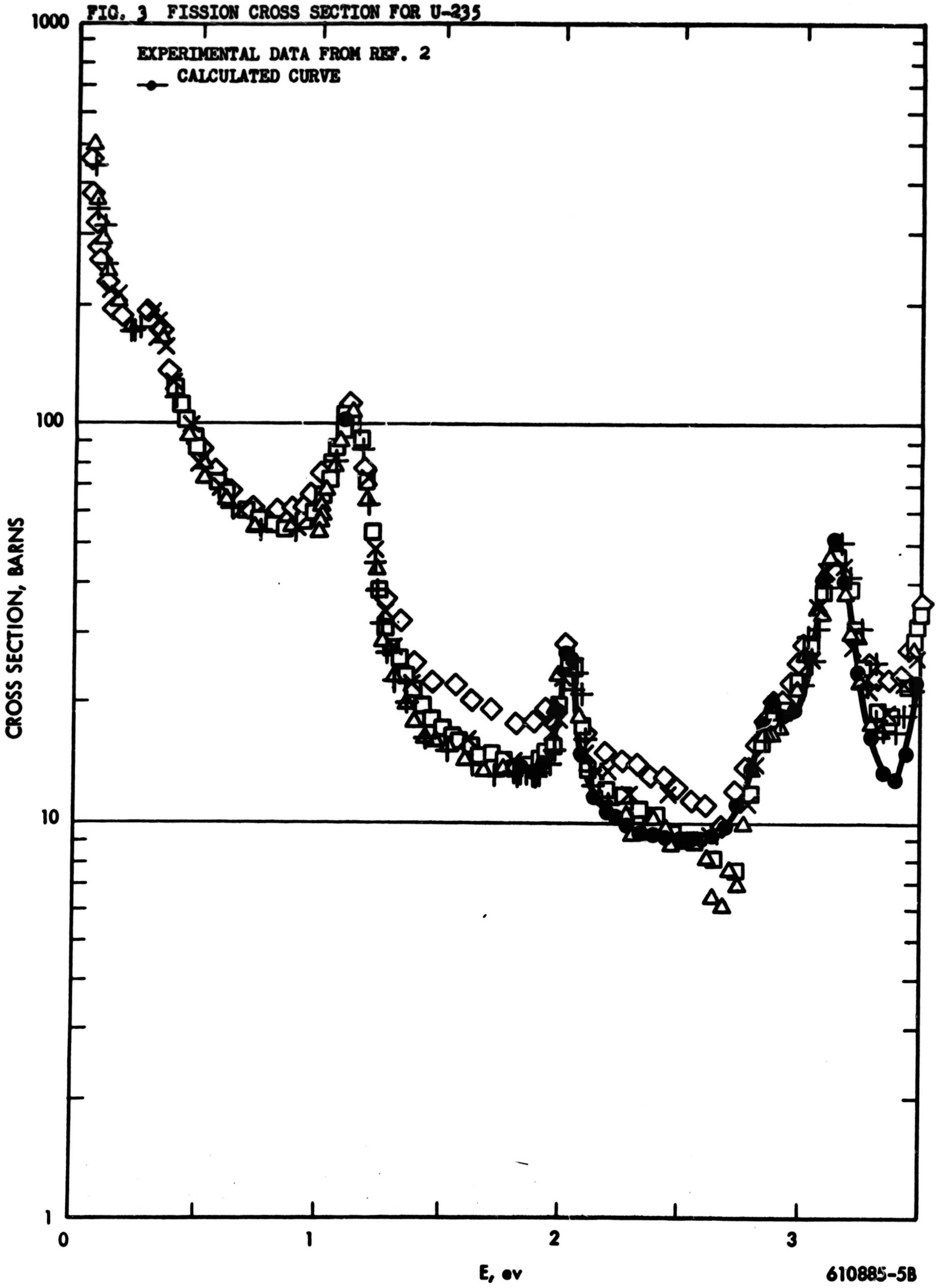

FIG. 4 FISSION CROSS SECTION FOR U-235

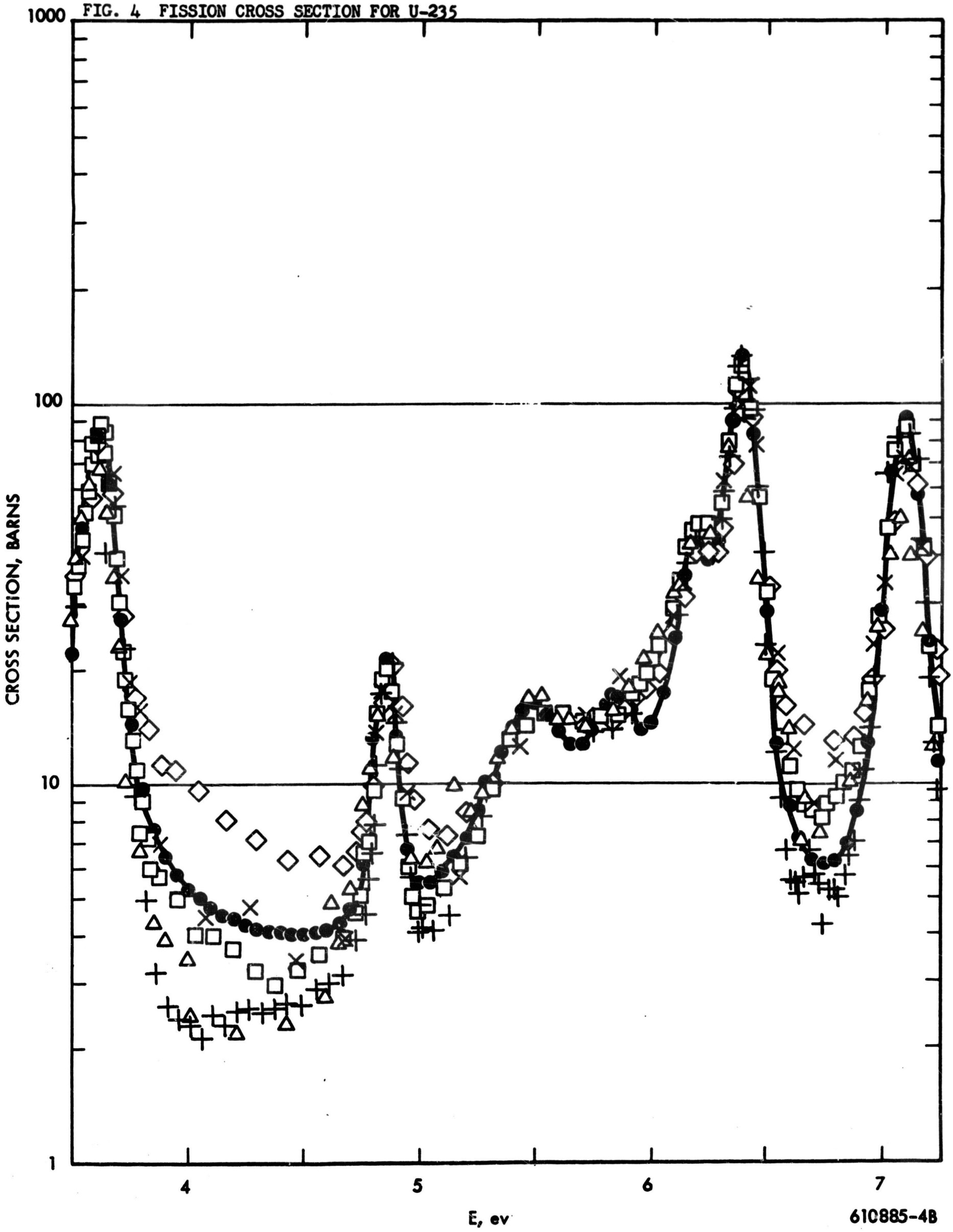

FIG. 5 FISSION CROSS SECTION FOR U-235

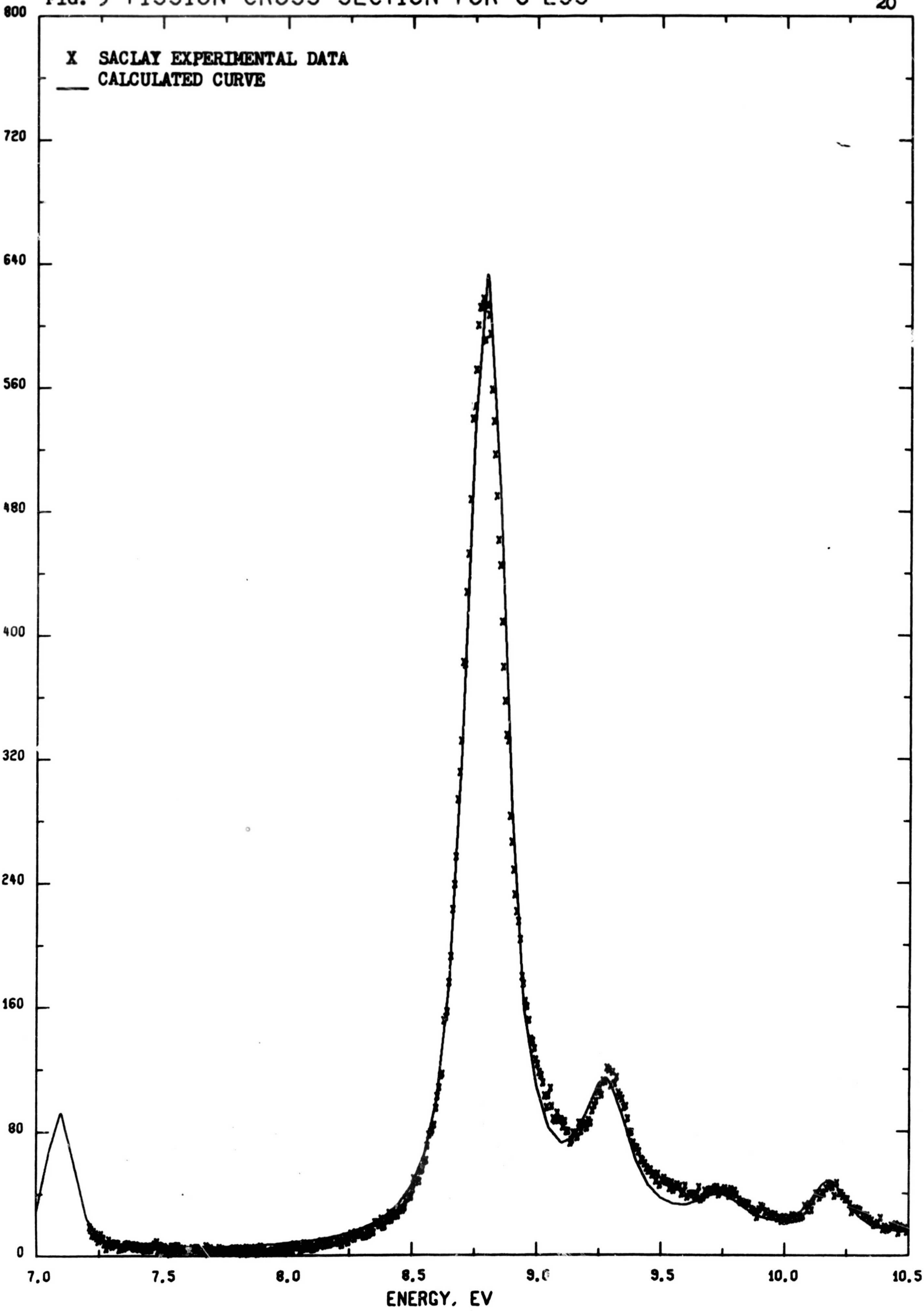

FIG. 6 FISSION CROSS SECTION FOR U-235

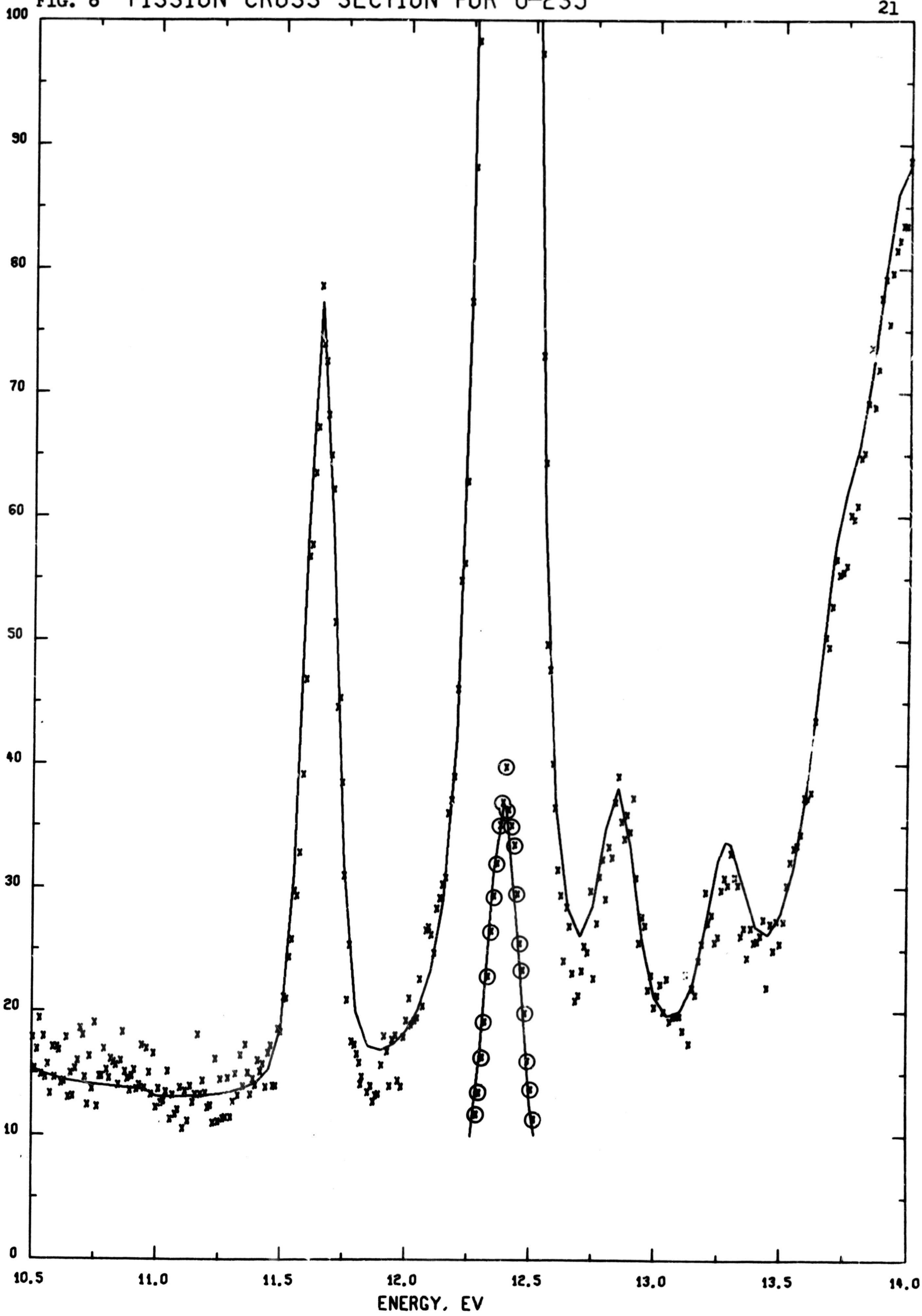

FIG. 7 FISSION CROSS SECTION FOR U-235

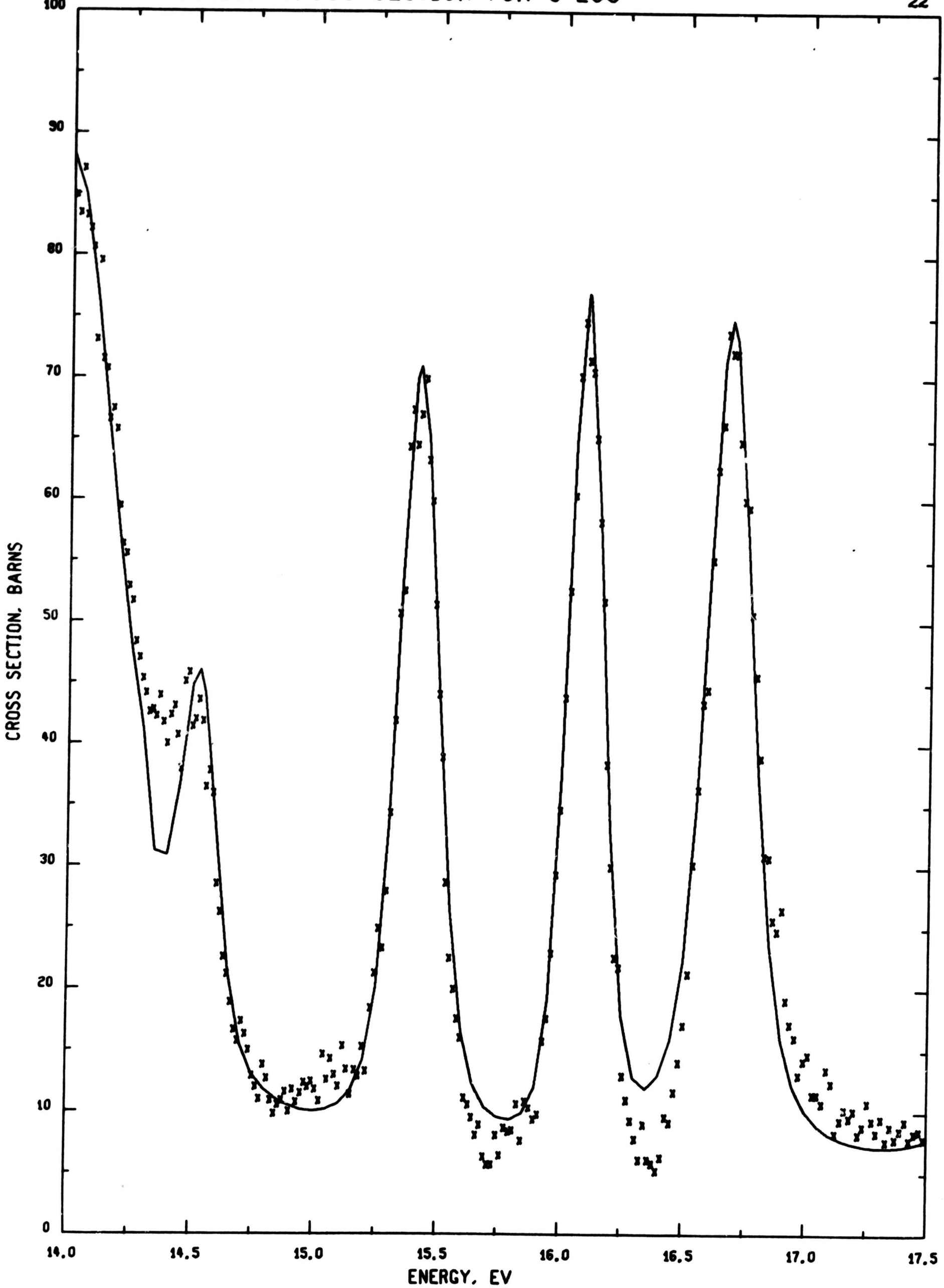

FIG. 8 FISSION CROSS SECTION FOR U-235

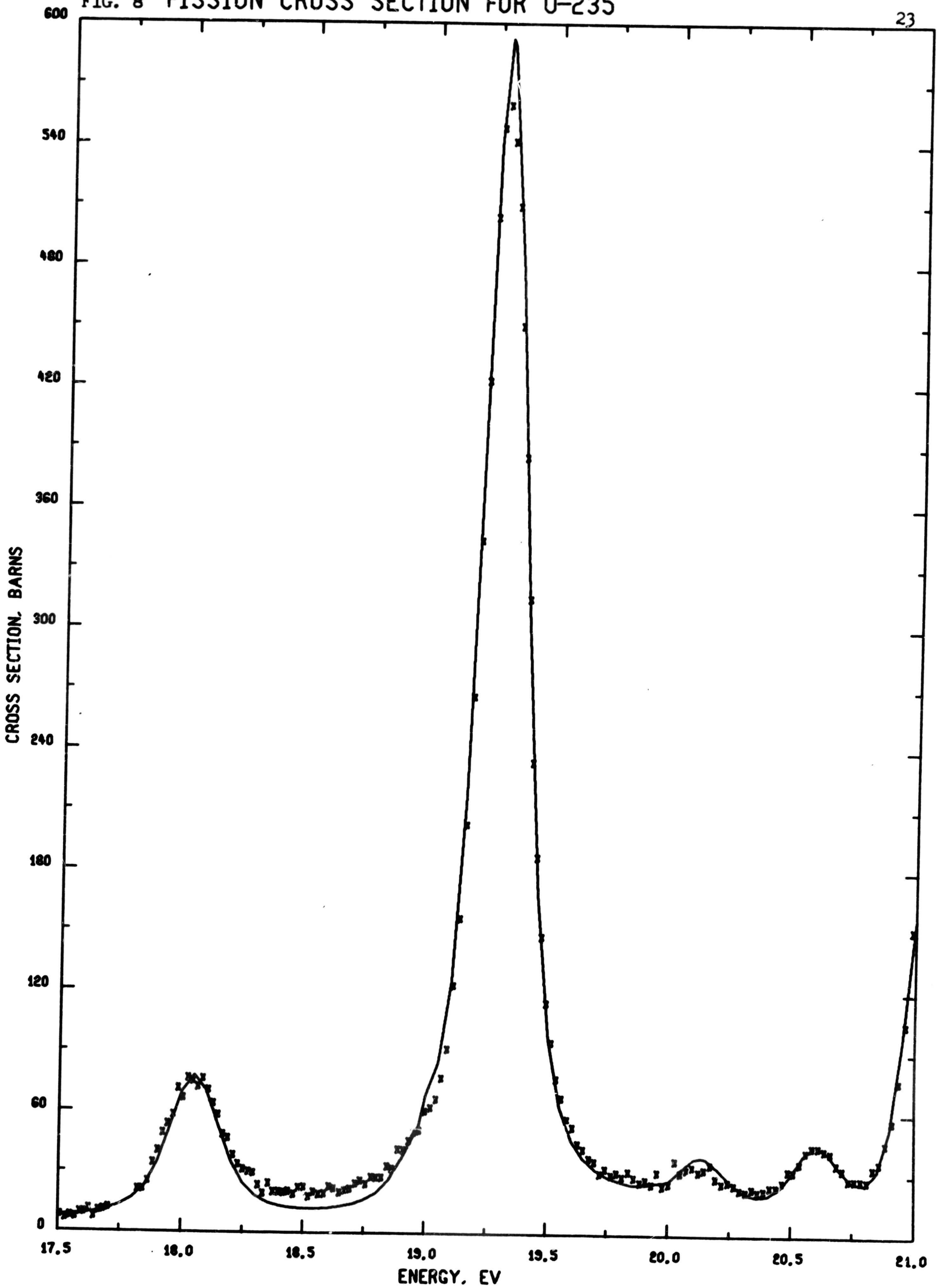

FIG. 9 FISSION CROSS SECTION FOR U-235

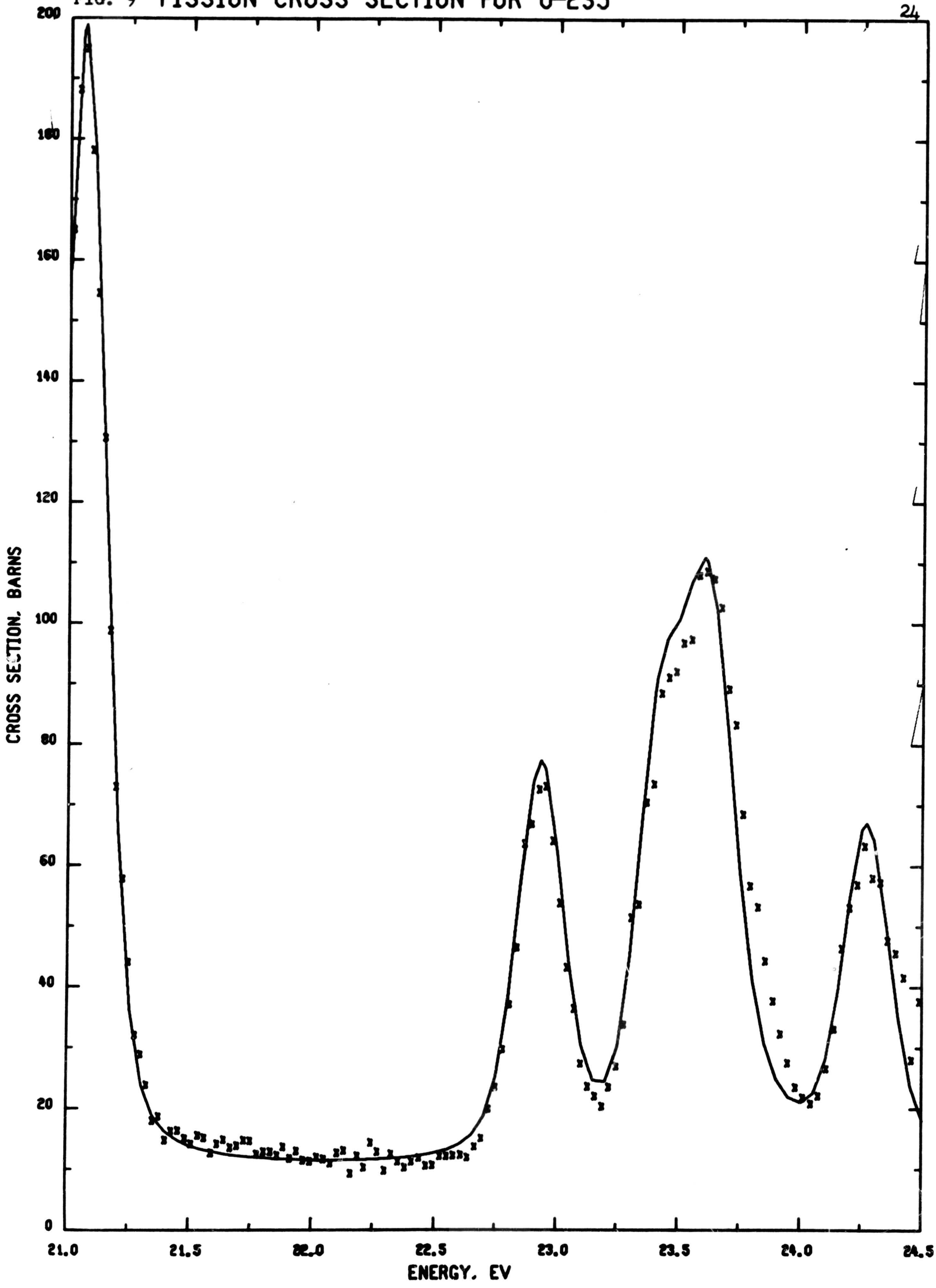

FIG. 10 FISSION CROSS SECTION FOR U-235

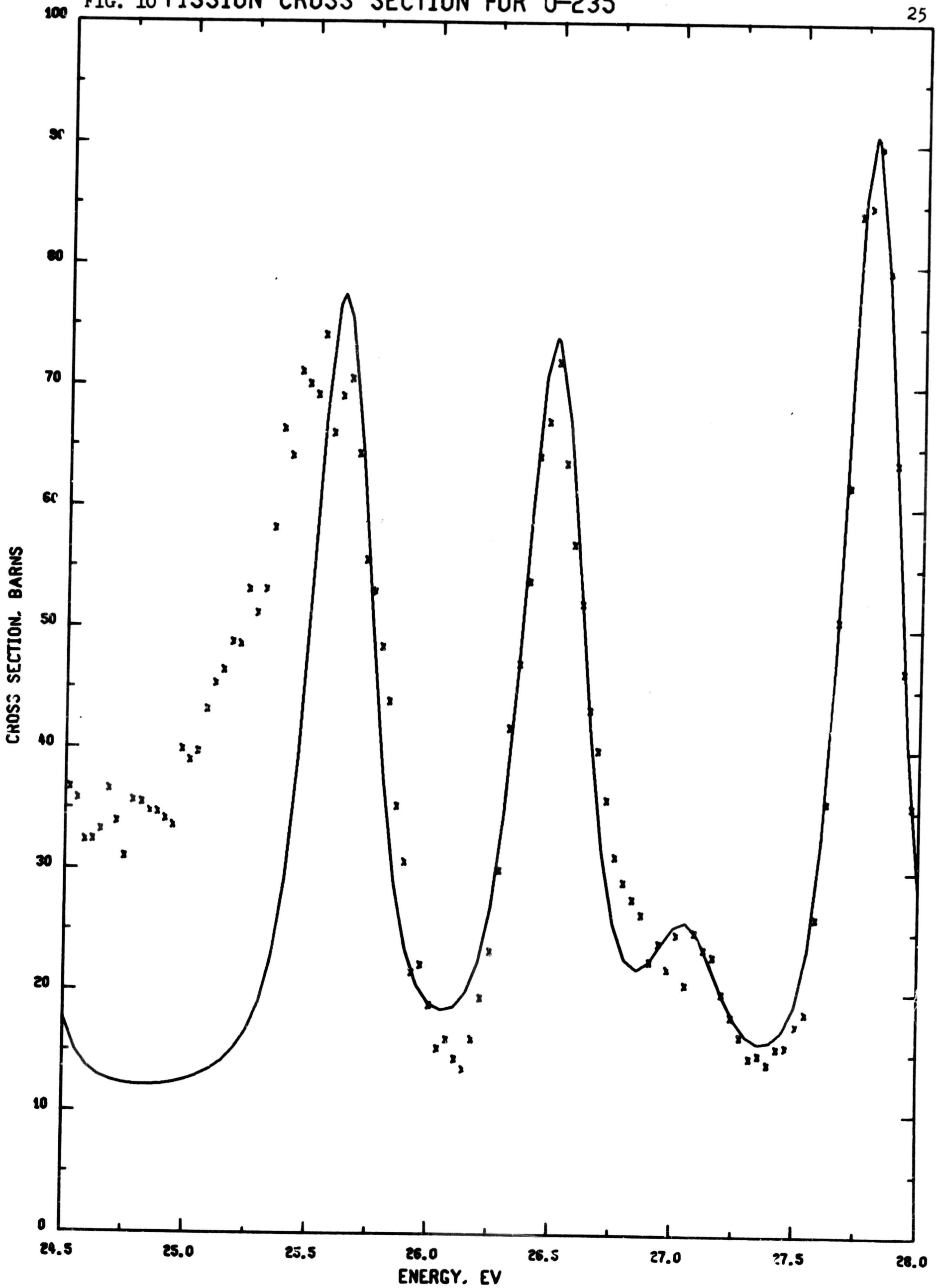

FIG. 11 FISSION CROSS SECTION FOR U-235

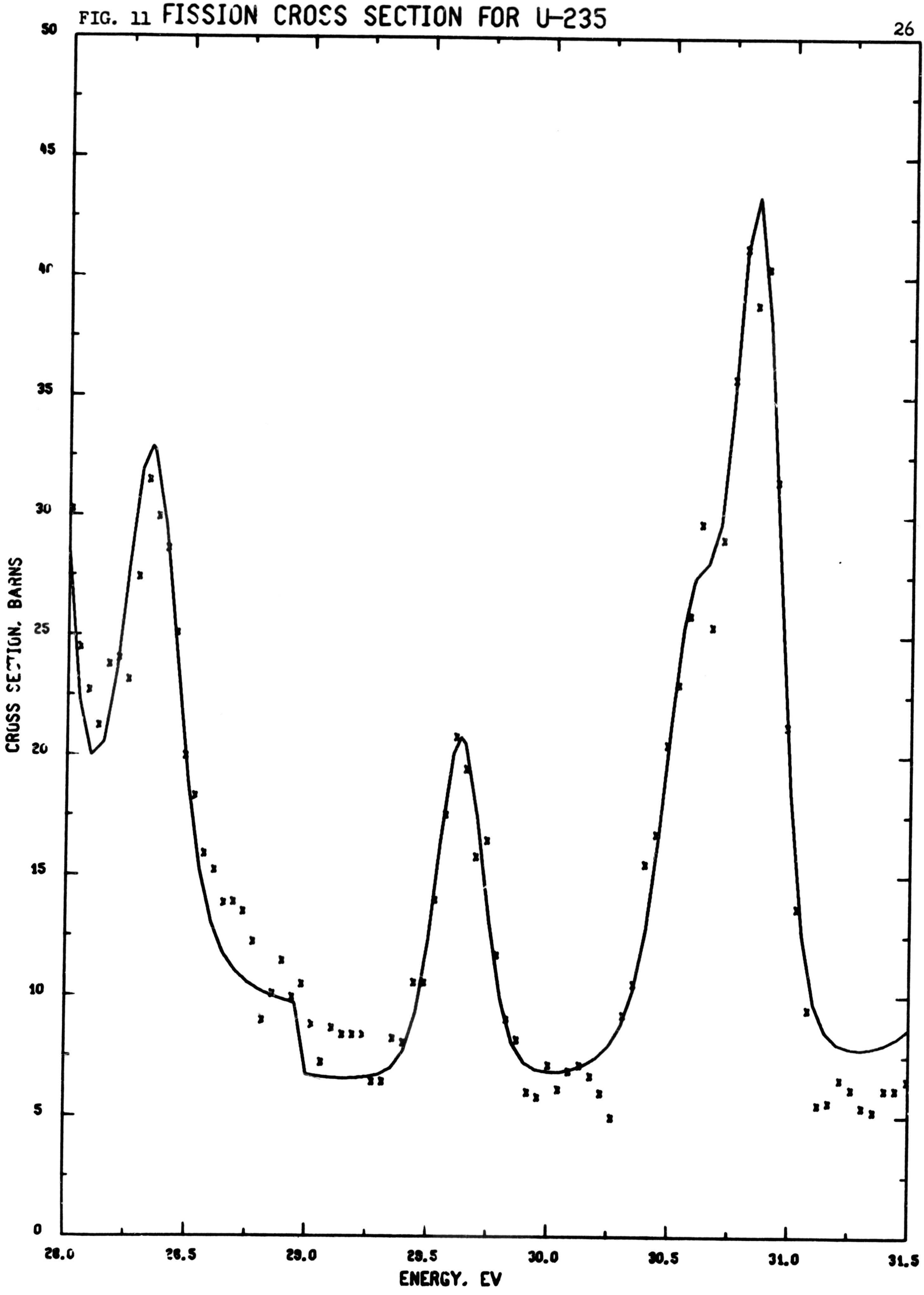

FIG. 12 FISSION CROSS SECTION FOR U-235

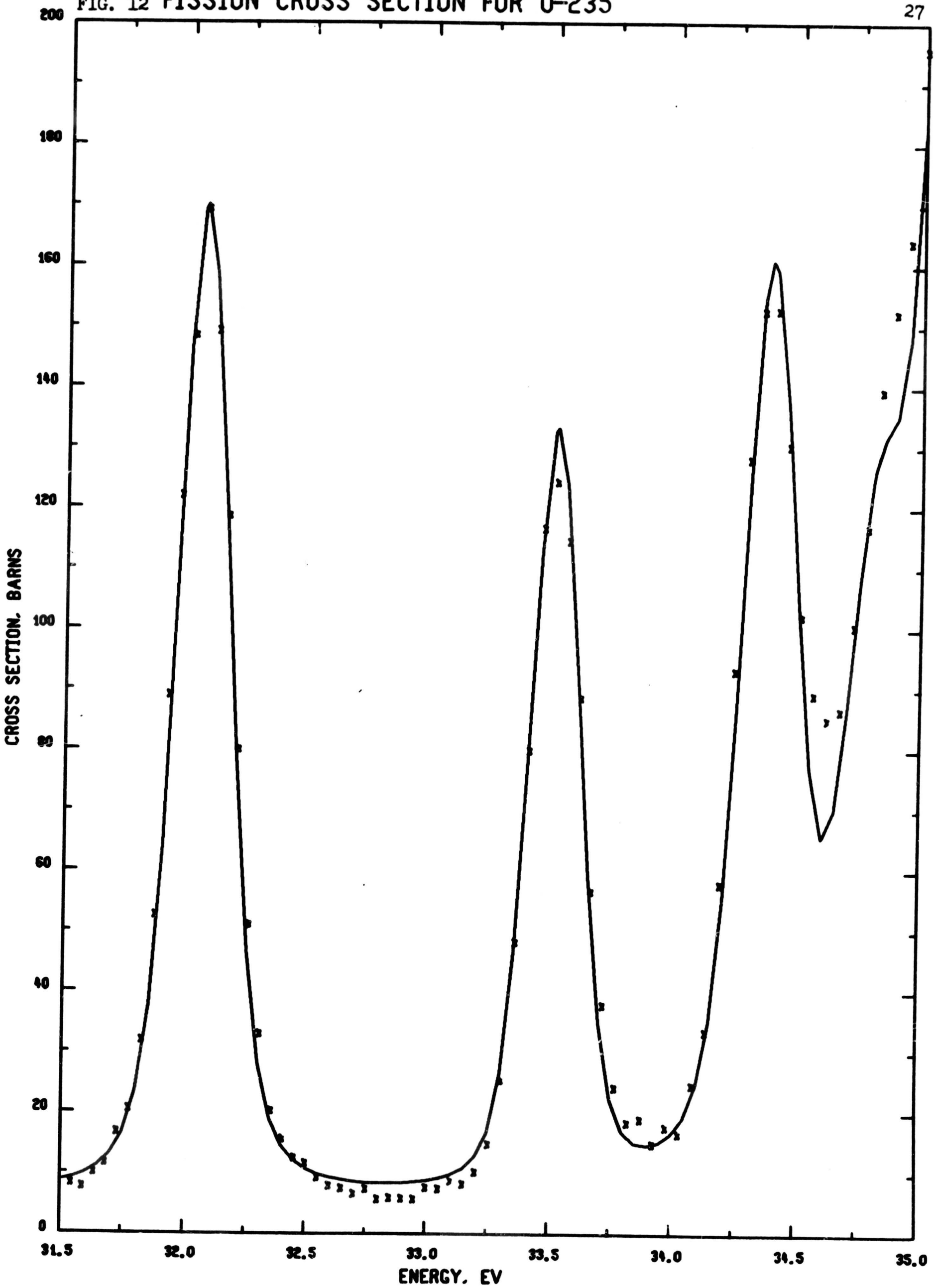

FIG. 13 FISSION CROSS SECTION FOR U-235

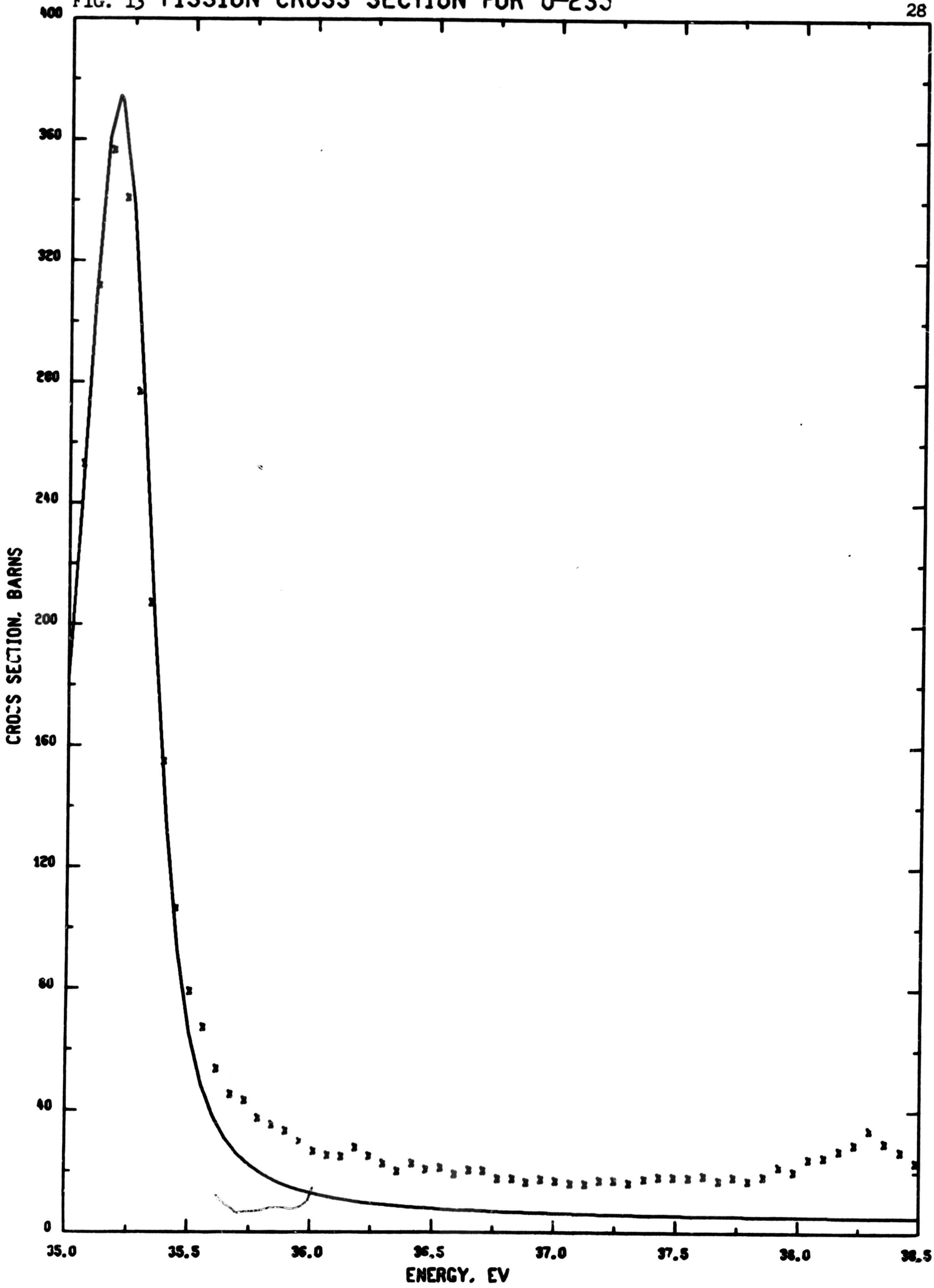

FIG. 14 TOTAL CROSS SECTION FOR U-235

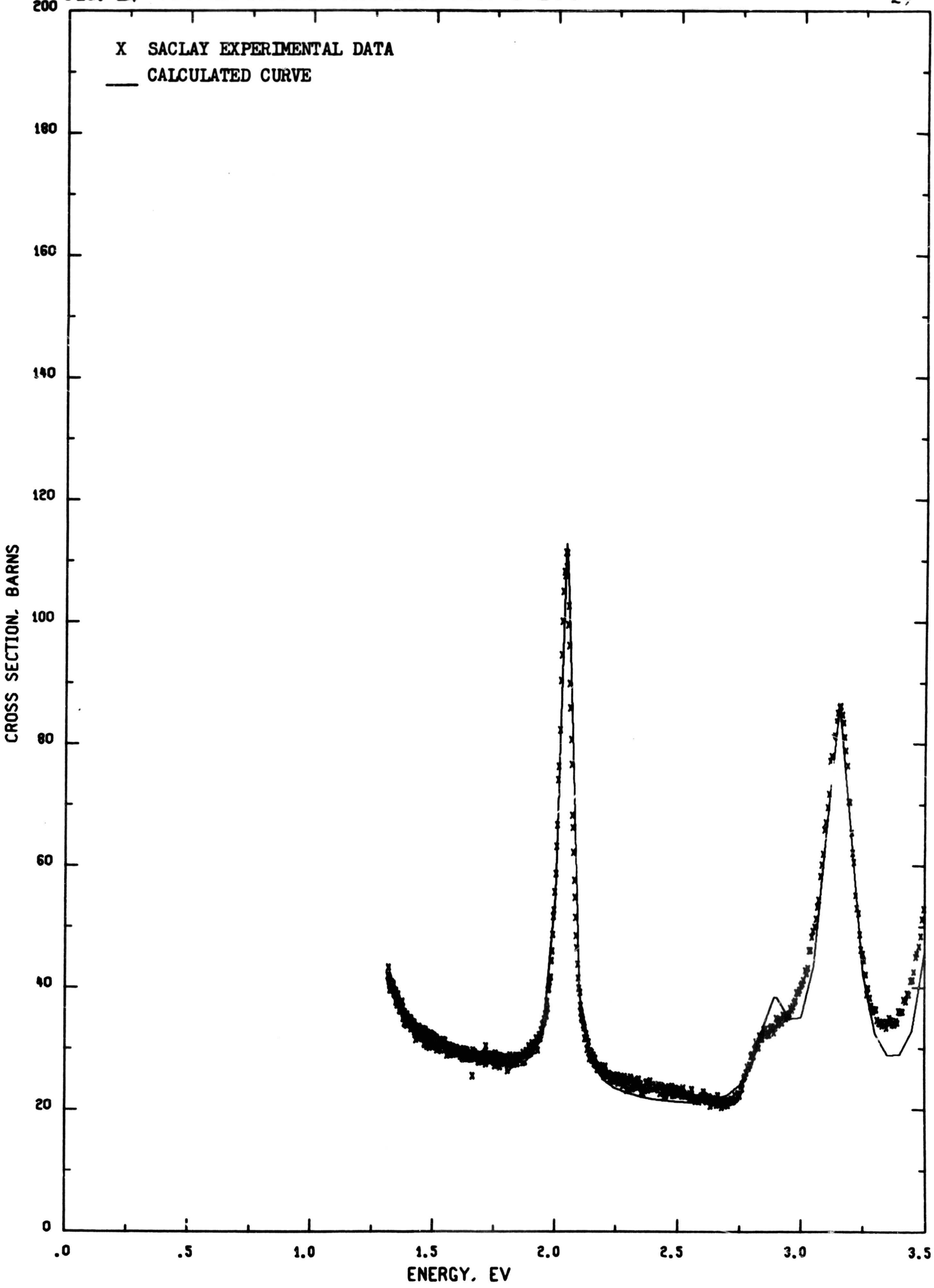

FIG. 15 TOTAL CROSS SECTION FOR U-235

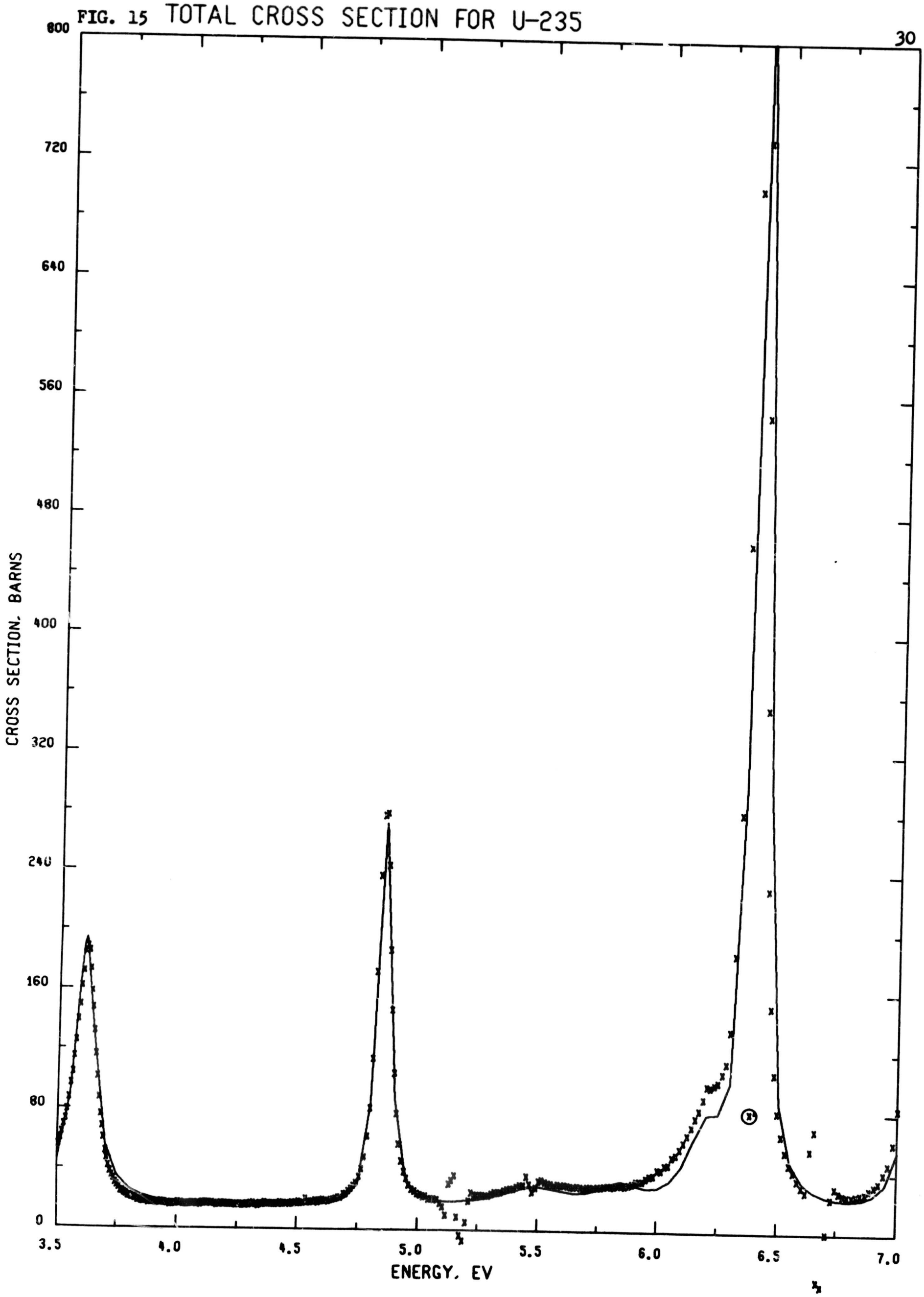

FIG. 16 TOTAL CROSS SECTION FOR U-235

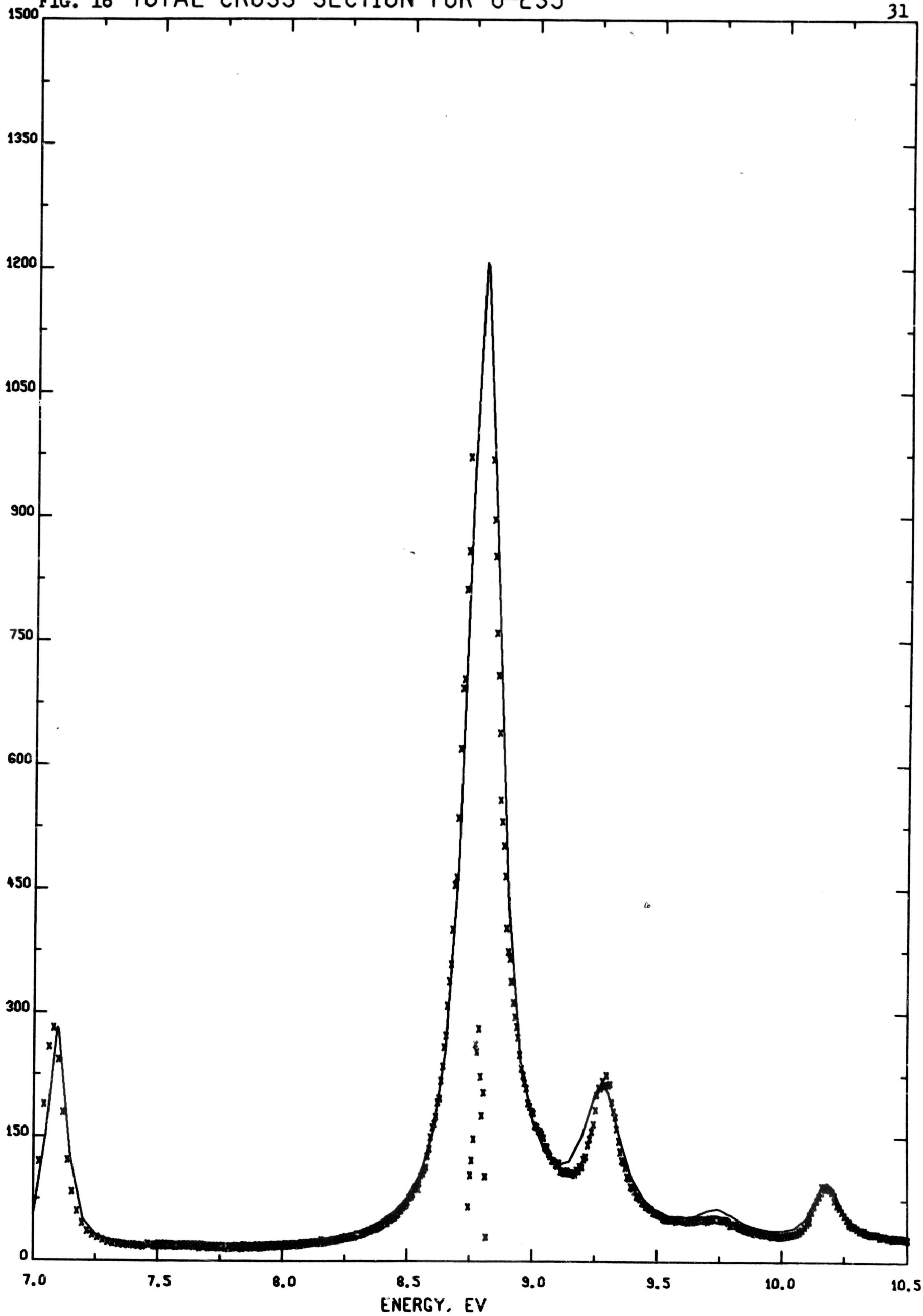

FIG. 17 TOTAL CROSS SECTION FOR U-235

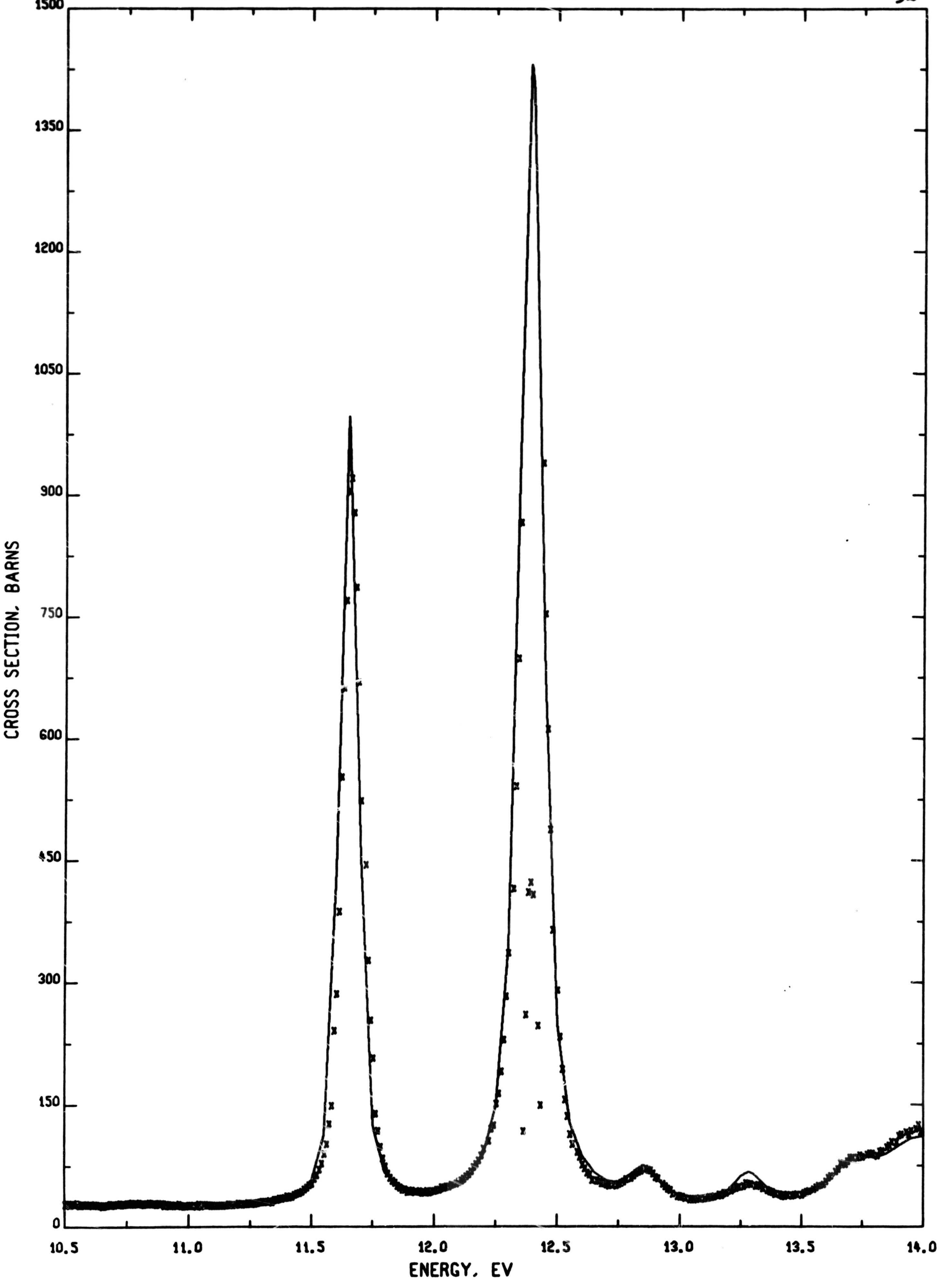

FIG. 18 TOTAL CROSS SECTION FOR U-235

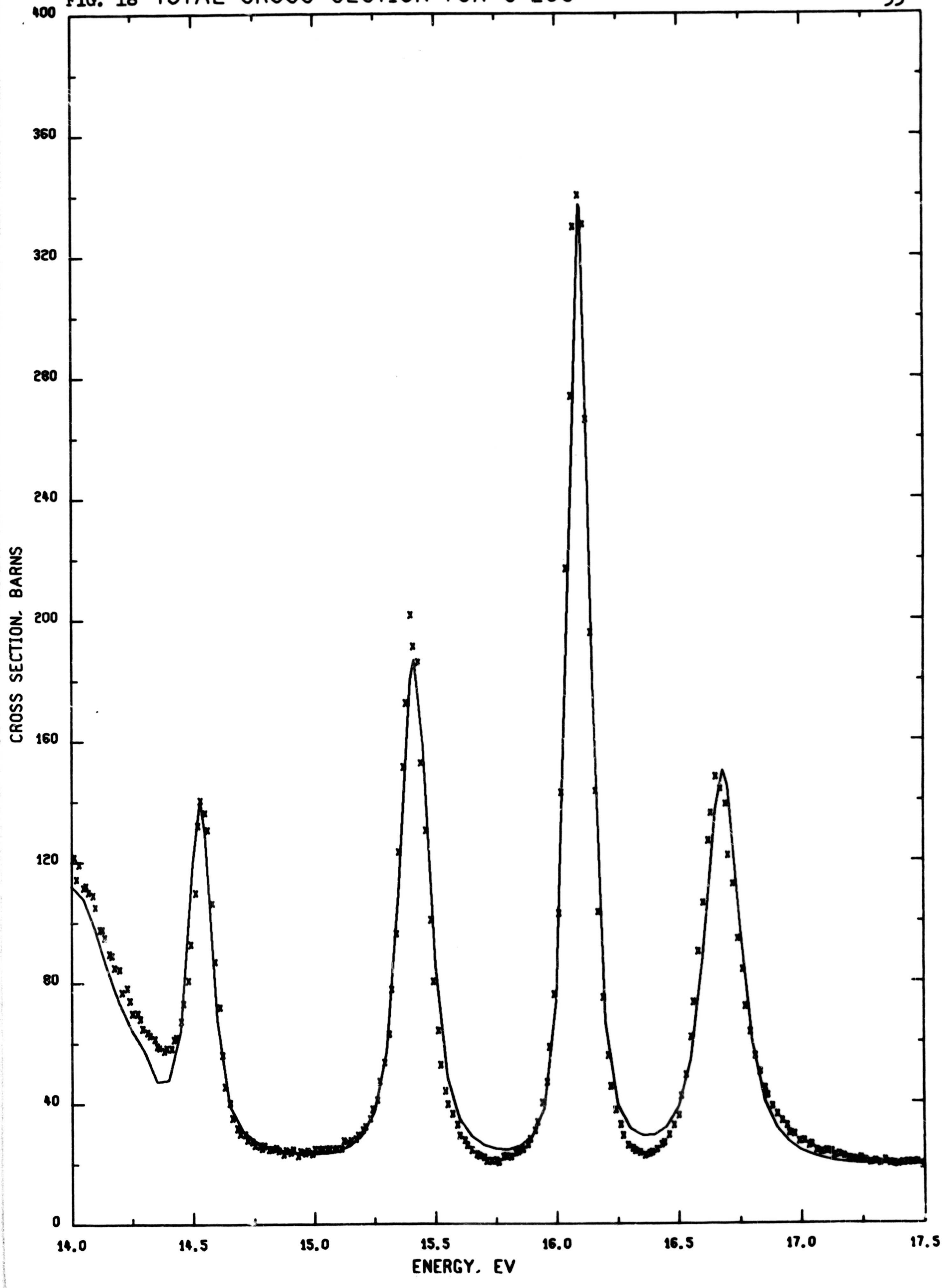

FIG. 19 TOTAL CROSS SECTION FOR U-235

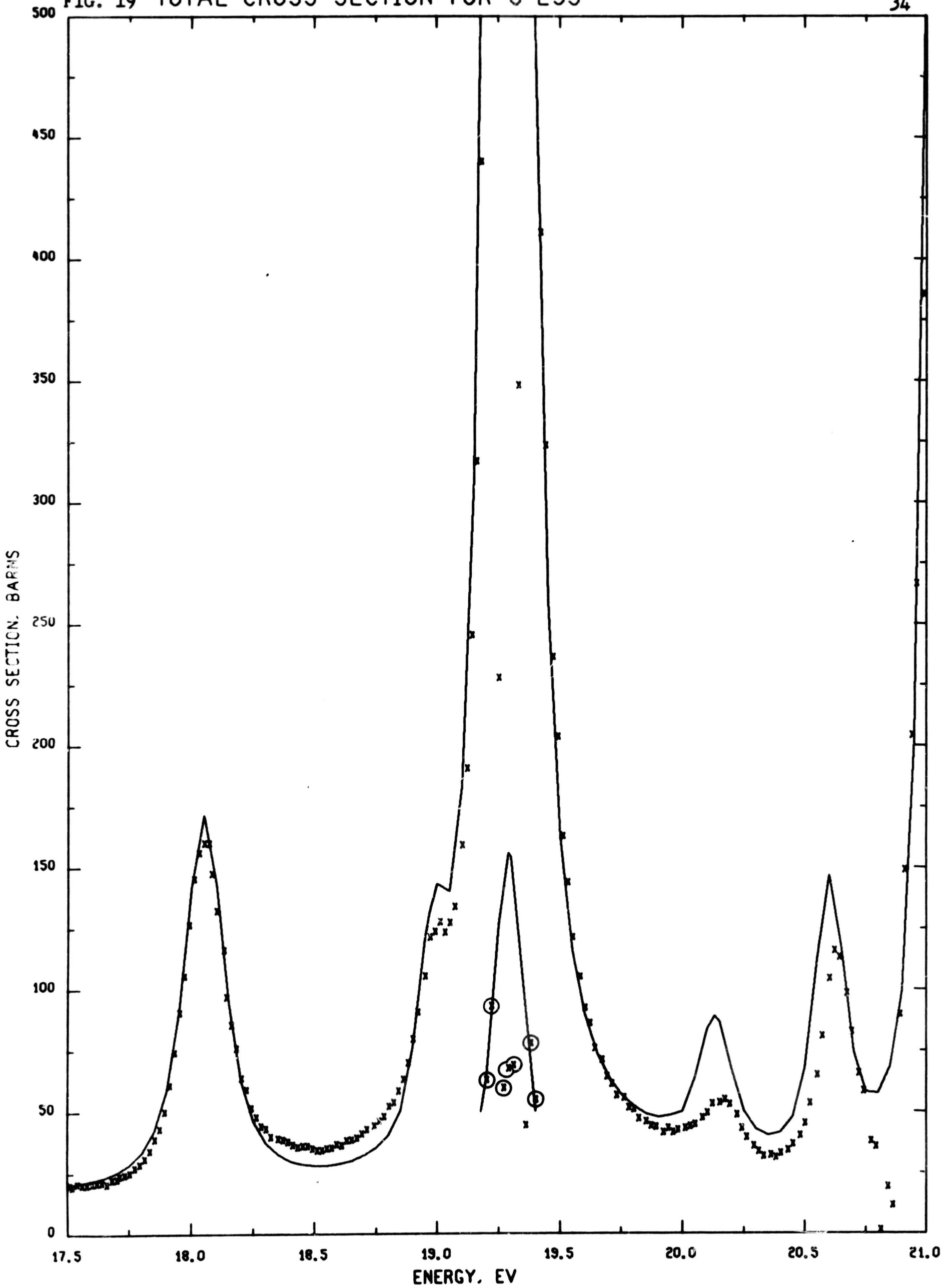

FIG. 20 TOTAL CROSS SECTION FOR U-235

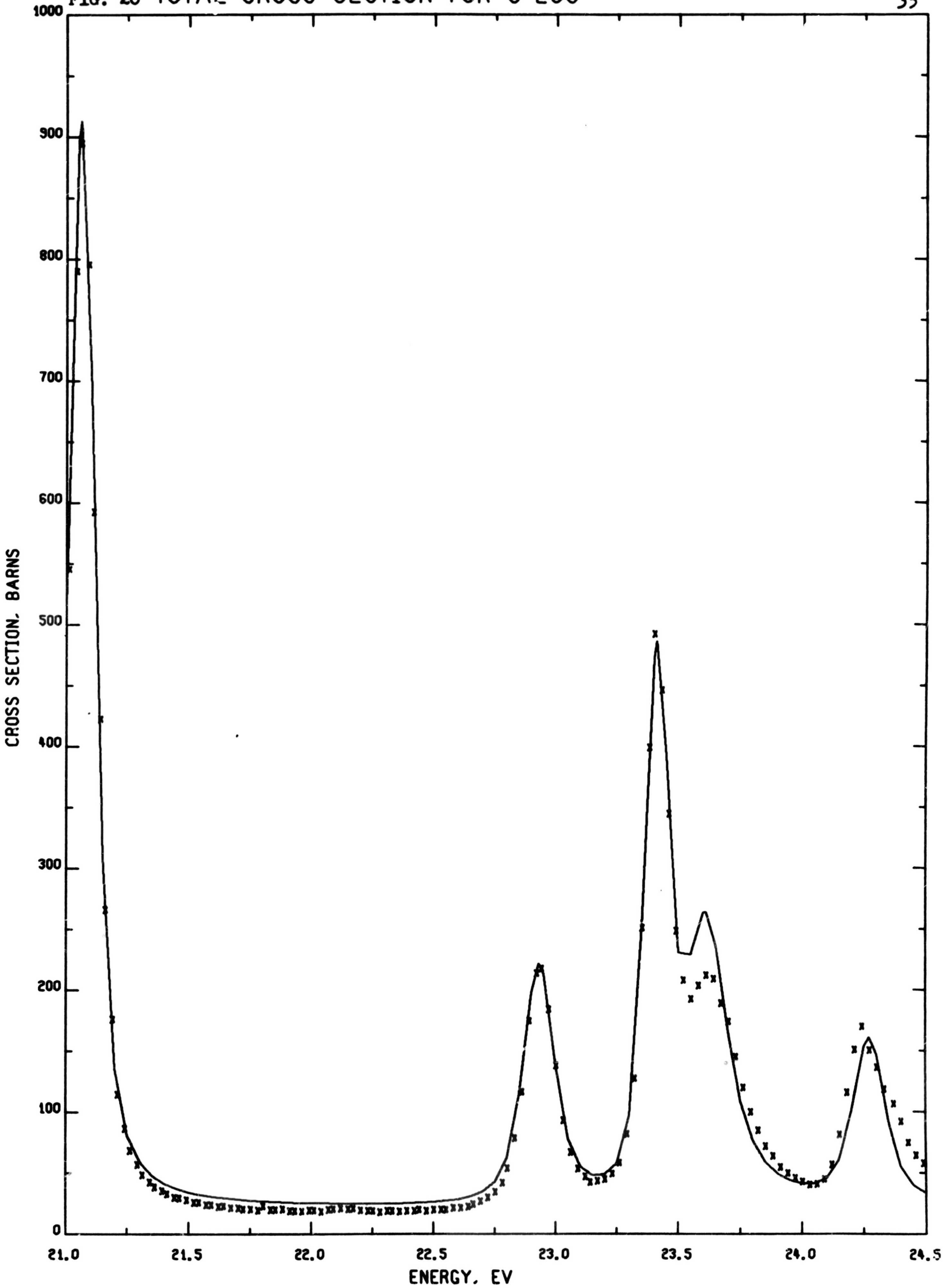

FIG. 21 TOTAL CROSS SECTION FOR U-235

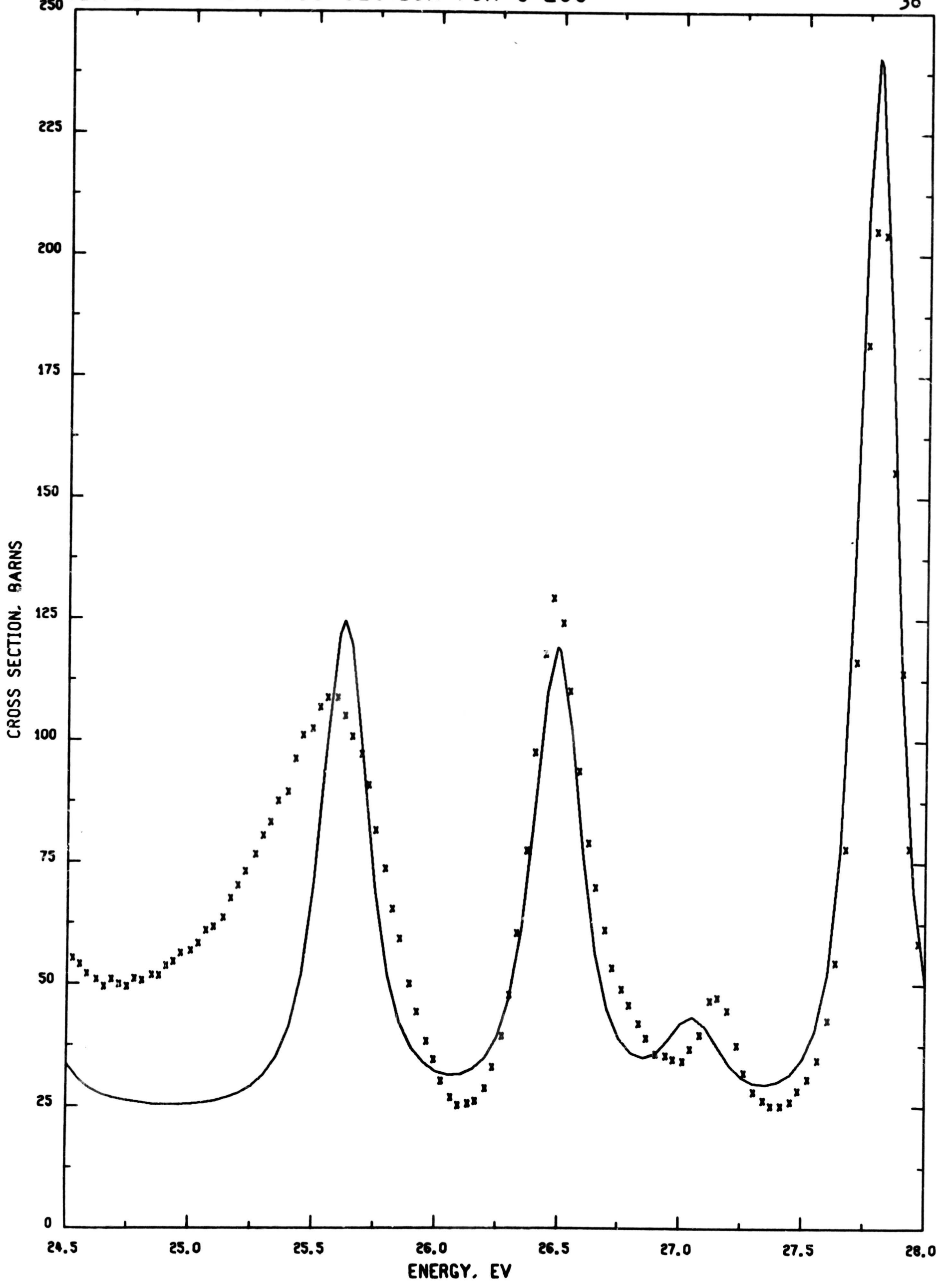

FIG. 22 TOTAL CROSS SECTION FOR U-235

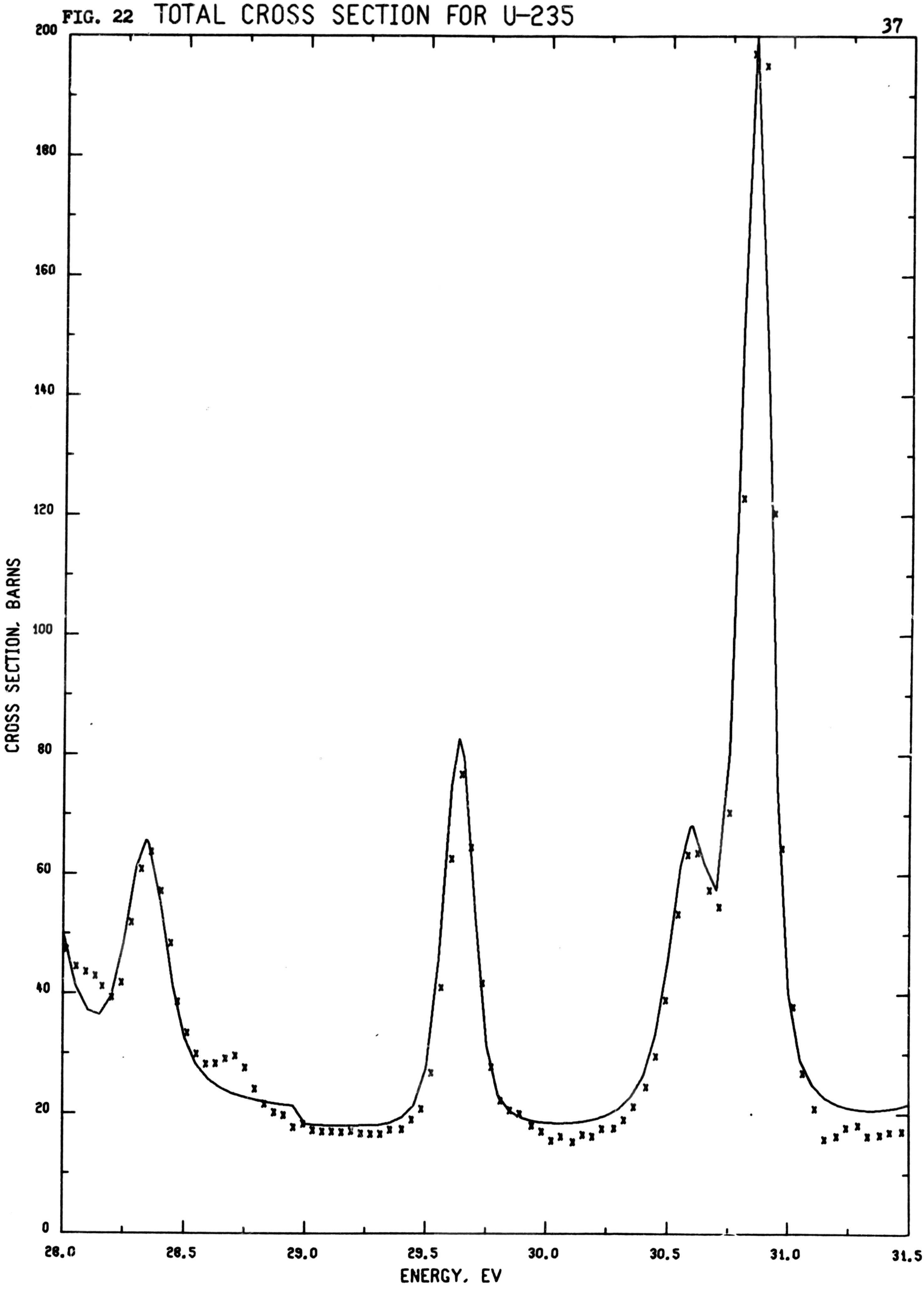

FIG. 23 TOTAL CROSS SECTION FOR U-235

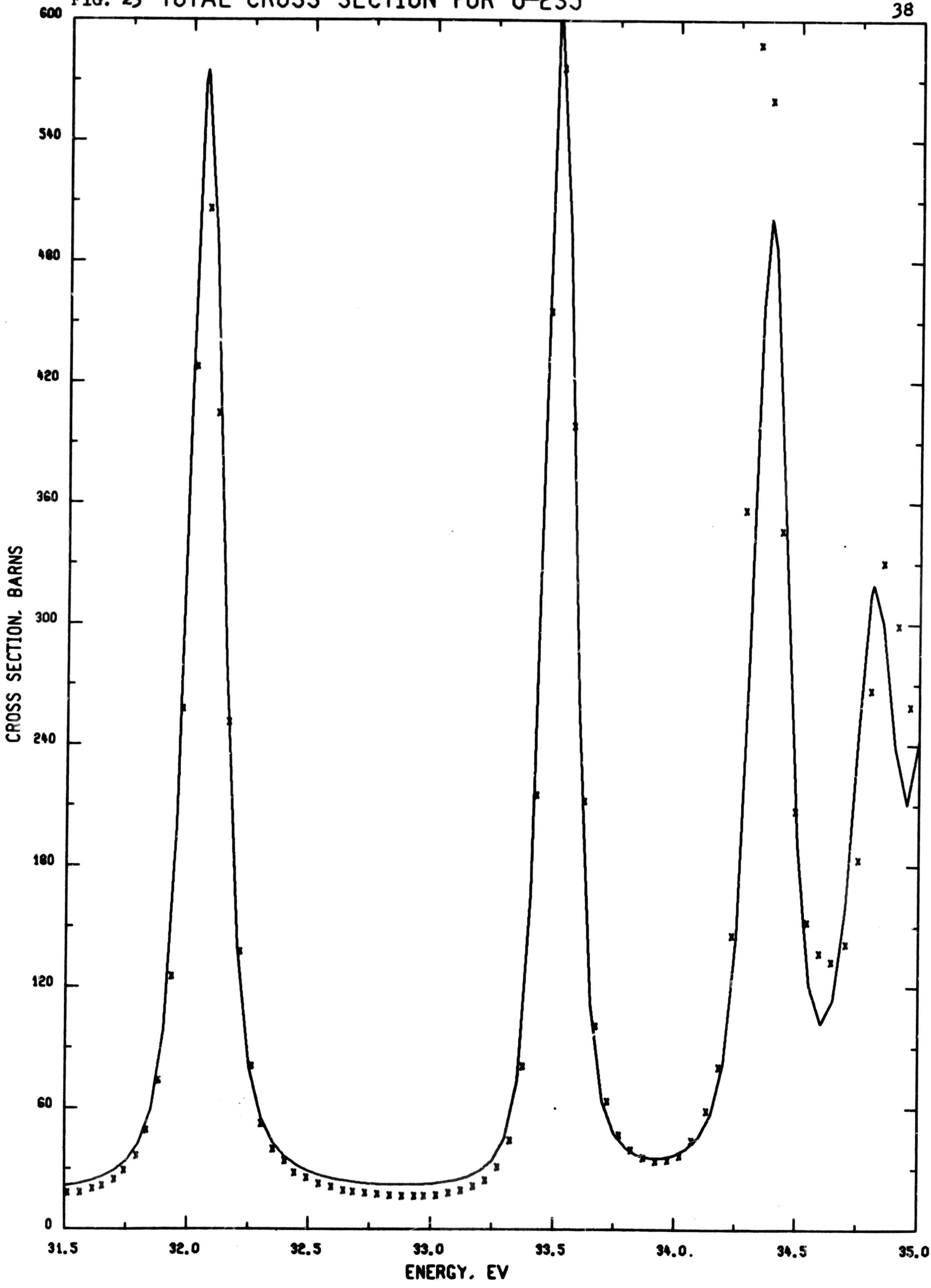

FIG. 24 TOTAL CROSS SECTION FOR U-235

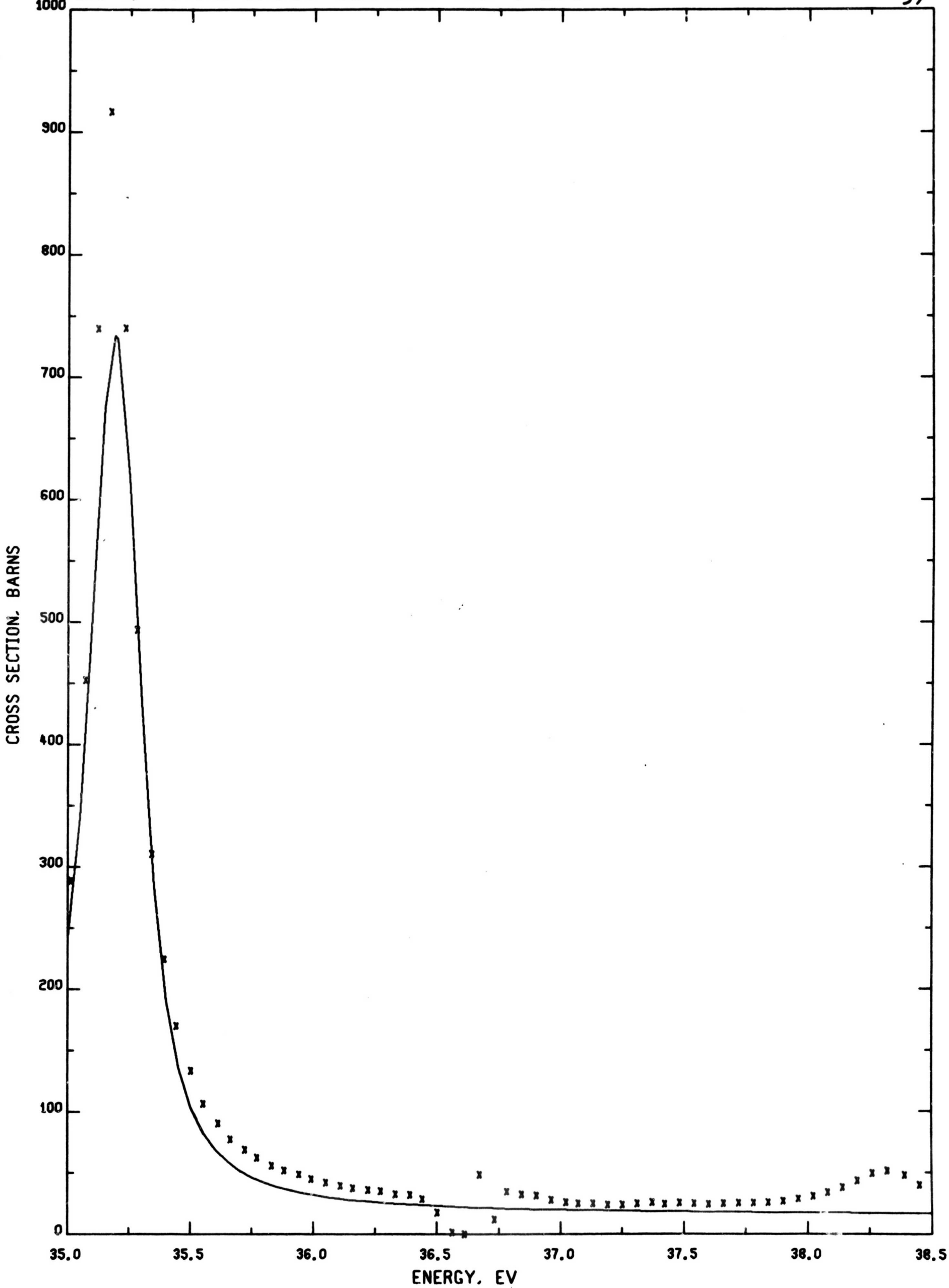

REFERENCES

1. A. Michaudon, CEA-R-2552 (Thesis, University of Paris), 1964.

2. Neutron Cross Sections, BNL-325 (Second Edition), Supplement 2, February 1965.

3. D. W. Drawbaugh, G. Gibson, and M. M. Melnick, A New Cross Section Library for the n + U^{235} Reactions, WANL-TME-1028, November 1964.

4. G. Gibson, W. H. Gray, and M. M. Melnick, Changes in the GAM-TNS Program and Cross Section Library, WANL-TME-1228, August 1965.

5. J. M. Friedman, and M. Platt, BNL-883(T-357), 1964.

6. G. Gibson and M. M. Melnick, XO and EXT, IBM-7094 Programs for Computing: (a) The Resonance Cross Sections for a Zero Temperature Target(XO), (b) The Maxwellian Doppler Broadened Breit-Wigner Resonances(EXT), WANL-TME-1132, March 1965. The set of equations solved by EXT are similar to those solved by the program TEWA described in the report: J. J. Devaney, et.al., LAMS-3075, May 1964.

7. E.g., see W. E. Lamb, Phys. Rev. 55, 190 (1939).

8. The results obtained under this approximation can be found in: A. M. Weinberg and E. P. Wigner, The Physical Theory of Neutron Chain Reactors, University of Chicago Press (1958) or L. Dresner, Resonance Absorption in Nuclear Reactors, Pergamon Press (1960).

9. A. Michaudon, General Survey on Methods of Theoretical Analysis of Data in Neutron Time-of-Flight Methods, Proceedings of Symposium published by Euratom, Brussels (1961).

10. E.g., see W. W. Havens and E. Melnonian, Peaceful Uses of Atomic Energy, U. N. Geneva 15, P/655, p.99 (1958).

11. M. M. Melnick, Curve Plot for SCISRS, WANL-TME-1317, November 1965.

12. H. J. Groenewold and Geoemdyk, Physica 13, 141 (1947).